

Chiral NCN Pincer Iridium(III) Complexes with Bis(imidazoliny)phenyl Ligands: Synthesis and Application in Enantioselective C–H Functionalization of Indoles with α -Aryl- α -diazoacetates

Nan Li, Wen-Jing Zhu, Juan-Juan Huang, Xin-Qi Hao, Jun-Fang Gong,* and Mao-Ping Song*

Cite This: <https://dx.doi.org/10.1021/acs.organomet.0c00174>

Read Online

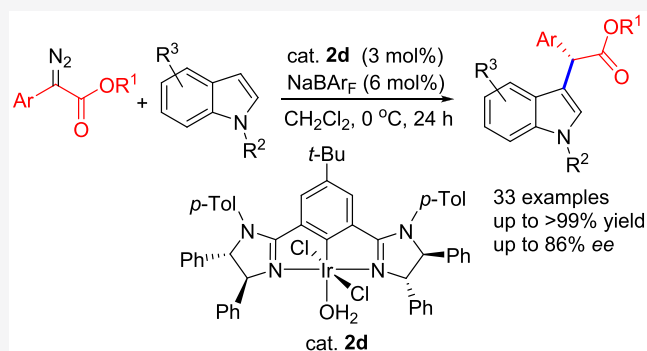
ACCESS |

Metrics & More

Article Recommendations

Supporting Information

ABSTRACT: A series of chiral NCN pincer iridium(III) complexes **2a–h** with bis(imidazoliny)phenyl ligands were synthesized via the central aryl C–H bond activation of the 1,3-bis(2'-imidazoliny)benzene ligands. The incorporation of a *tert*-butyl group into the central aryl ring of the ligands was found to markedly improve the efficiency of the desired C2-metalation, leading to an obvious enhancement in the yields of the Ir(III) complexes. Consequently, complexes with a *tert*-butyl group on the central aryl ring were obtained in 34–47% yields, whereas those without the group were produced in only 13–16% yields. All of the new complexes have been characterized by elemental analysis and ^1H and $^{13}\text{C}\{^1\text{H}\}$ NMR spectroscopy. In addition, the molecular structures of complexes **2c**, **2d**, and **2g'** have been determined by X-ray single-crystal diffraction. **2c** and **2d** are, indeed, the anticipated six-coordinate pincer Ir(III) complexes. In contrast, **2g'** is a coordinatively unsaturated five-coordinate pincer Ir(III) complex. The Ir(III) complexes were used as the catalysts for the asymmetric C–H insertion reaction of α -aryl- α -diazoacetates with *N*-protected indoles. With a catalyst loading of 3 mol % and in the presence of 6 mol % of NaBAR_F , a variety of optically active indole derivatives bearing chiral functional groups at the C3 position were obtained in good yields with moderate to good enantioselectivities (up to 86% *ee*).



INTRODUCTION

Organometallic pincer iridium complexes, which contain a meridionally tridentate ligand, have been applied to a wide variety of stoichiometric and catalytic chemical transformations including, among others, C–H bond activation, C–O bond cleavage, olefin hydroaryloxylation, monoisomerization of 1-alkenes to *trans*-2-alkenes, α -alkylation of unactivated esters with primary alcohols, (de)hydrogenation and transfer (de)hydrogenation reactions, as well as tandem reactions involving alkane dehydrogenation (AD).^{1,2} The high thermal stability of the pincer Ir complexes afforded by the tridentate coordination mode and their high modularity are the two key factors responsible for their successful applications in various transformations. In particular, the PCP-type Ir complexes based on the motif of a central coordinating carbanion and two flanking P-coordinating groups have been systematically investigated and found to be highly active, regioselective, and thermally robust catalysts for alkane dehydrogenation and the related tandem reactions. Despite the fact that the PCP pincer Ir complex-catalyzed alkane dehydrogenation is very efficient, the active site for the C–H activation of the alkane, which is believed to be an Ir(I) species, is often inhibited by the

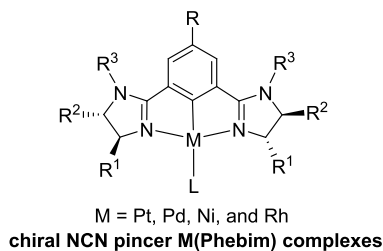
presence of N_2 , water, or the olefin product. Therefore, the development of non-PCP-type pincer Ir catalysts for AD has been increasingly gaining research interest in the past several years. In this regard, research from the groups of Nishiyama, Goldberg, Goldman, and Jones have demonstrated that the NCN-type Ir complexes with a bis(oxazoliny)phenyl ligand (2,6-bis(4,4-dimethyloxazoliny)-3,5-dimethylphenyl, abbreviated as *dm*Phebox) are particularly promising, even though their applications are currently limited to being stoichiometric.^{2a,3} For these NCN Ir complexes, C–H activation of the alkane occurs at an Ir(III) center, which is in sharp contrast with the Ir(I)-based PCP catalysts. Consequently, the stoichiometric AD mediated by the NCN Ir complexes is not inhibited by either N_2 or olefin and rather is accelerated by water.

Received: March 10, 2020

As described above, the dm Phebox ligand complexed with Ir to form the NCN pincer (dm Phebox)Ir complexes that showed great potentials in alkane dehydrogenation. Additionally, the Phebox ligand is also an ideal ligand skeleton for the introduction of chirality, which can be readily achieved by using commercially available and optically active amino alcohols as a chiral source, leading to the construction of chiral NCN pincer (Phebox)Ir complexes. In fact, as early as in 2006, Nishiyama and coworkers reported the first synthesis of this type of complex.^{4,5} A rather preliminary investigation of the application of the chiral (Phebox)Ir complex in asymmetric catalysis indicated that the complex exhibited only moderate activity with good enantioselectivity in the asymmetric conjugate reduction of an α,β -unsaturated ester (63% yield with 72% *ee*) and the reductive aldol reaction of *tert*-butyl acrylate with benzaldehyde (48% yield with 89% *ee*).⁴ In 2013, Musaev, Davies, Blakey, and coworkers synthesized a series of chiral (Phebox)Ir complexes with varied electronic and steric properties. From this small library of complexes, the optimal catalyst for the asymmetric C–H insertion reaction of α -aryl- α -diazoacetates with 1,4-cyclohexadiene was screened and successfully identified, giving the desired products in generally high yields and with high enantioselectivities (up to 99% yield and 99% *ee*).⁶

We have been interested in developing new chiral pincer complexes for applications in metal-catalyzed enantioselective transformations.⁷ For this purpose, we have designed and synthesized various NCN pincer metal including Pt, Pd, Ni, and Rh complexes with chiral bis(imidazolyl)phenyl ligands (abbreviated as Phebim, Chart 1).⁸ The Phebim ligand can be

Chart 1



viewed as a structural analogue of the Phebox ligand, of which the oxygen atom in the oxazoline ring is replaced by a NR^3 group. Similar to the Phebox ligands, the chiral moiety in the Phebim ligands can be readily introduced and tuned by using different chiral amino alcohols, which is beneficial for obtaining the optimal catalysts. More importantly, the NR^3 group is clearly different from the O atom in electronic and steric properties, which may bring about enhanced reactivity or stereoselectivity of the complexes with Phebim ligands. In particular, the changeable feature of the R^3 substituent in the NR^3 group provides an additional opportunity to modulate the reactivity and stereoselectivity of the corresponding pincer complexes. Works from our laboratory^{7,8} and other groups of Duan⁹ and Nakamura¹⁰ have shown that these complexes displayed good activities with good to excellent enantioselectivities in the Pt-catalyzed Friedel–Crafts alkylation of indoles with nitroalkenes,^{7c,8d} the Rh-catalyzed allylation of aldehydes, the carbonyl-ene reaction and alkynylation of trifluoropyruvates^{7c,8e,f} as well as the Pd-catalyzed hydrophosphination of enones,^{7c,d,8g,9} the allylation of ketimines, and reactions of several types of nitrile compounds with

sulfonimines.^{7d,10} In particular, Musaev, Sigman, Davies, Blakey, and coworkers have successfully applied the chiral (Phebim)Ir complexes to enantioselective C–H insertion reactions of ethyl diazoacetate into phthalan and dihydrofuran derivatives (up to 96% *ee*).¹¹ The study also clearly showed that both the yield and enantioselectivity of the catalysis product were influenced by the NR^3 group to varying degrees. By choosing an appropriate R^3 substituent, the corresponding (Phebim)Ir complex was then able to afford a better enantioselectivity than the related (Phebox)Ir complex.

Despite the enduring prominent role of the achiral pincer iridium complexes in homogeneous catalysis, the synthesis and applications of chiral ones have, in contrast, received much less attention and effort.^{4,6,11} Therefore, to fully explore the organometallic chemistry of chiral pincer Ir complexes, and also as a part of our effort to expand further our previous work, we herein report the synthesis and characterization of a series of new chiral NCN pincer (Phebim)Ir complexes as well as their use as catalysts for the enantioselective C–H functionalization of indoles with α -aryl- α -diazoacetates.

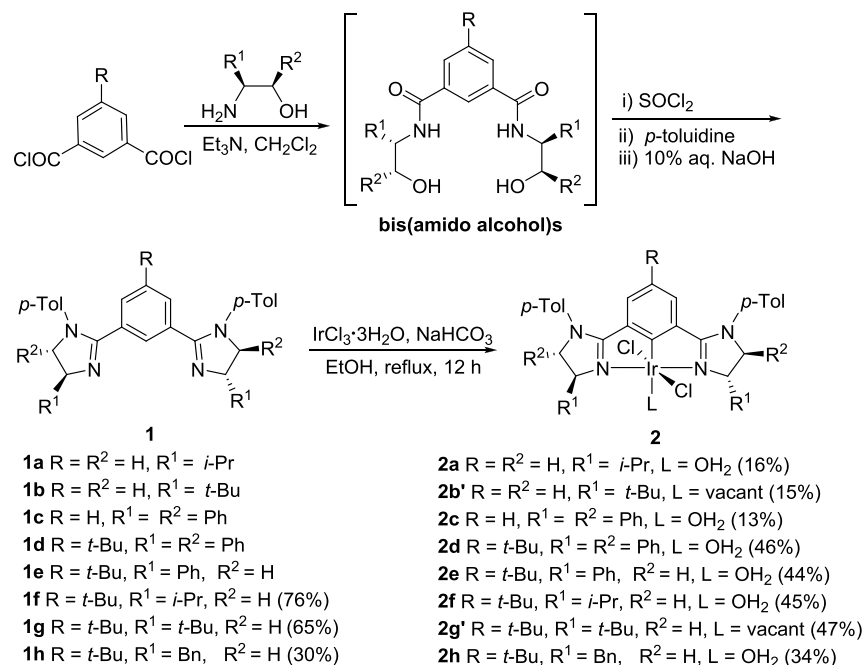
RESULTS AND DISCUSSION

Synthesis and Characterization of the Chiral NCN Pincer (Phebim)Ir Complexes. As shown in Scheme 1, the required Phebim pincer ligand precursors, 1,3-bis(2'-imidazolyl)benzene (Phebim-H) ligands **1a–h**, were conveniently synthesized from isophthaloyl dichloride or 5-*tert*-butyl isophthaloyl dichloride according to the procedure we previously reported.⁸ First, reactions of the dichlorides with several chiral amino alcohols including *L*-valinol, *L*-*tert*-leucinol, (1*R*,2*S*)-2-amino-1,2-diphenylethanol, *L*-phenylglycinol, and *L*-phenylalaninol afforded the corresponding bis(amido alcohol)s. Next, the eight crude bis(amido alcohol) products were, without further purification, allowed to react with thionyl chloride and *p*-toluidine successively, followed by treatment with aqueous NaOH. During the process, chlorination (twice), amination, and cyclization to imidazoline occurred smoothly in sequence to give rise to the desired Phebim-H ligands **1a–h**. Among the obtained eight ligands, the ligands **1f–h** are new compounds, and the other five are known.

With the chiral ligands **1** in hand, synthesis of the pincer Ir(III) complexes via central aryl C2–H bond activation of the ligands was tried by reaction of the ligands with iridium(III) chloride trihydrate in the presence of sodium hydrogen carbonate in refluxing ethanol. It was found that the expected chiral NCN pincer iridium(III) complexes **2a–c** were successfully obtained, albeit in rather low yields (13–16%). In contrast, the complexes **2d–h** with a *tert*-butyl group on the central aryl ring were produced in acceptable yields (34–47%). The obviously higher yields of **2d–h** are likely due to the steric effect of a bulky *tert*-butyl group that promotes the desired C2-metalation by hindering the undesired C4- or C6-metalation in the reaction of the ligands **1d–h** with the Ir(III) salt.

All of the above new pincer (Phebim)Ir complexes were characterized by ¹H NMR, ¹³C{H} NMR, and elemental analysis. The ¹H NMR spectra of complexes **2a**, **2c–f**, and **2h** showed a singlet (commonly a broad singlet) integrated for two protons in the range of 1.87 to 3.11 ppm, which was assigned to the metal-coordinated H₂O protons, whereas for complexes **2b'** and **2g'**, the corresponding singlets were not observed, suggesting the absence of the coordinated H₂O molecule. Elemental analysis results of these complexes confirmed that their molecular formulations were consistent

Scheme 1. Synthesis of the Chiral NCN Pincer Iridium(III) Complexes 2a–h with Bis(imidazolyl)phenyl Ligands



with the structures shown in Scheme 1. That is, **2b'** and **2g'** are five-coordinate complexes without the coordination of H₂O, and the others are the expected H₂O-bound six-coordinate complexes. In addition, the molecular structures of **2c**, **2d**, and **2g'** were unambiguously determined by X-ray single-crystal diffraction analysis. The molecules with selected bond lengths and angles are shown in Figures 1–3, respectively. Complexes **2c** and **2d** are six-coordinate pincer complexes with meridionally tridentate coordination of the

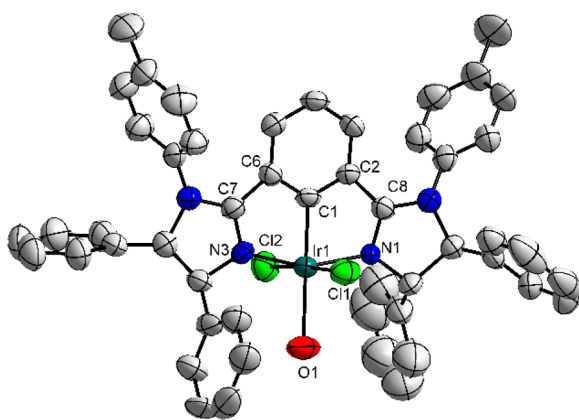


Figure 1. Molecular structure of complex **2c** with thermal ellipsoids drawn at the 50% probability level. (Hydrogen atoms are omitted for clarity; one of the two independent molecules is shown.) Selected bond lengths (Å) and angles (deg): Ir(1)–C(1) 1.939(7), Ir(1)–N(1) 2.039(6), Ir(1)–N(3) 2.033(6), Ir(1)–O(1) 2.264(6), Ir(1)–Cl(1) 2.345(2), Ir(1)–Cl(2) 2.347(3), C(1)–Ir(1)–O(1) 178.4(3), N(1)–Ir(1)–N(3) 158.4(3), C(1)–Ir(1)–N(1) 79.3(3), C(1)–Ir(1)–N(3) 79.1(3), C(1)–Ir(1)–Cl(1) 89.6(3), C(1)–Ir(1)–Cl(2) 93.7(3), N(1)–Ir(1)–Cl(1) 86.7(2), N(1)–Ir(1)–Cl(2) 94.6(2), N(1)–Ir(1)–O(1) 100.9(3), N(3)–Ir(1)–Cl(1) 91.8(2), N(3)–Ir(1)–Cl(2) 88.0(2), N(3)–Ir(1)–O(1) 100.6(3), O(1)–Ir(1)–Cl(1) 88.8(2), O(1)–Ir(1)–Cl(2) 87.9(2), Cl(1)–Ir(1)–Cl(2) 176.62(9).

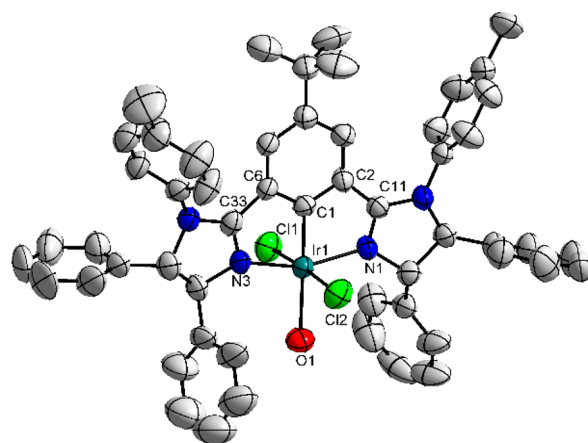


Figure 2. Molecular structure of complex **2d**·C₈H₈·C₆H₆ with thermal ellipsoids drawn at the 50% probability level. (Hydrogen atoms and solvent molecules are omitted for clarity.) Selected bond lengths (Å) and angles (deg): Ir(1)–C(1) 1.936(8), Ir(1)–N(1) 2.069(6), Ir(1)–N(3) 2.060(6), Ir(1)–O(1) 2.293(7), Ir(1)–Cl(1) 2.347(3), Ir(1)–Cl(2) 2.337(3), C(1)–Ir(1)–O(1) 179.2(3), N(1)–Ir(1)–N(3) 158.3(3), C(1)–Ir(1)–N(1) 79.4(3), C(1)–Ir(1)–N(3) 78.9(3), C(1)–Ir(1)–Cl(1) 92.2(3), C(1)–Ir(1)–Cl(2) 93.2(3), N(1)–Ir(1)–Cl(1) 92.6(3), N(1)–Ir(1)–Cl(2) 87.8(3), N(1)–Ir(1)–O(1) 101.3(3), N(3)–Ir(1)–Cl(1) 89.0(3), N(3)–Ir(1)–Cl(2) 92.6(3), N(3)–Ir(1)–O(1) 100.4(3), O(1)–Ir(1)–Cl(1) 87.4(2), O(1)–Ir(1)–Cl(2) 87.1(2), Cl(1)–Ir(1)–Cl(2) 174.52(11).

Phehim ligand as well as coordination of a H₂O molecule and two chloride ligands to the Ir(III) center. The iridium(III) center in each complex features a distorted-octahedral geometry wherein the H₂O ligand is located in the pincer plane and the two chloride ligands are in a trans configuration. The Ir–C bond lengths in the two complexes are ~1.94 Å, and the N–Ir–N angles are 158.4(3) and 158.3(3)°, respectively, which are comparable to those in a related achiral (Phebox)Ir complex.⁴ The Ir–O bond lengths in complexes **2c** and **2d**

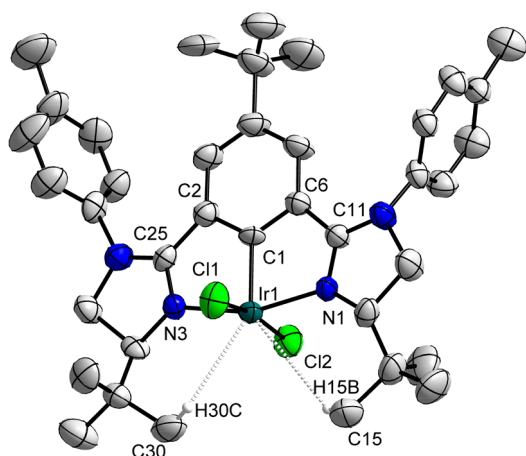


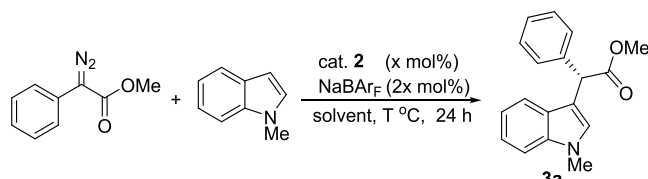
Figure 3. Molecular structure of complex **2g'** with thermal ellipsoids drawn at the 50% probability level. (Most hydrogen atoms are omitted for clarity; one of the two independent molecules is shown.) Selected bond lengths (Å) and angles (deg): Ir(1)–C(1) 1.891(6), Ir(1)–N(1) 2.057(5), Ir(1)–N(3) 2.059(6), Ir(1)–Cl(1) 2.323(2), Ir(1)–Cl(2) 2.333(2), N(1)–Ir(1)–N(3) 159.9(2), C(1)–Ir(1)–N(1) 79.9(3), C(1)–Ir(1)–N(3) 80.0(3), C(1)–Ir(1)–Cl(1) 98.2(2), C(1)–Ir(1)–Cl(2) 92.2(2), N(1)–Ir(1)–Cl(1) 87.21(19), N(1)–Ir(1)–Cl(2) 93.88(19), N(3)–Ir(1)–Cl(1) 94.90(19), N(3)–Ir(1)–Cl(2) 87.66(19), Cl(1)–Ir(1)–Cl(2) 169.53(9). Ir(1)⋯H(30C)–C(30) 2.792, Ir(1)⋯H(15B)–C(15) 2.984.

were found to be slightly longer than that in the (Phebox)Ir complex (2.264(6) to 2.293(7) Å vs 2.243 Å).⁴ In contrast with complexes **2c** and **2d**, complex **2g'** was found to be an uncommon five-coordinate pincer complex¹² with coordination of the Phebim ligand and two chloride ligands. Unlike complexes **2c** and **2d**, complex **2g'** is devoid of the coordination of a H₂O molecule and is coordinatively unsaturated. Its structure is notable for a square-based pyramidal geometry about the Ir(III) metal. This structural outcome is likely a result of steric shielding of the vacant coordination site by the *tert*-butyl groups of imidazole rings in the pincer ligand. Also notable, there exist weak Ir–H agostic interactions¹³ between the *tert*-butyl groups of imidazole rings and iridium, which might have a stabilizing effect on the Ir(III) center. The Ir⋯H–C distances (2.792–2.984 Å) are comparable to those in the related five-coordinate pincer Ir complexes (2.978(5)–3.072(3) Å).^{12b,c}

C–H Insertion of α -Aryl- α -diazoacetates with Indoles. Transition-metal-catalyzed asymmetric insertion reactions of metal carbenes, *in-situ*-generated from diazo compounds, into the C–H bonds have found broad applications in organic synthesis for C–H functionalization and the construction of C–C bonds.¹⁴ In this regard, the catalytic enantioselective C–H insertion of α -aryl- α -diazoacetates with indoles provides an efficient method for the synthesis of indoles bearing chiral functional groups at the C3 position that are common in many biologically active natural products and therapeutic agents. Several effective and stereoselective catalytic systems including Fe-chiral spiro bisoxazoline ligand (up to 78% *ee*),^{15a} Rh-chiral phosphoric acid (up to 94% *ee*),^{15b} and Pd- and Cu-axially chiral bipyridine ligand (up to 98% *ee* and 95% *ee*, respectively),^{15c,d} have been recently developed for this specific transformation. However, up to now, there have been no reports on the Ir-catalyzed enantioselective C–H insertion of α -aryl- α -diazoacetates with indoles, even though it has been demonstrated that some Ir

catalysts including pincer Ir catalysts performed very well in asymmetric carbene insertion into C–H bonds.^{6,11,16} We speculated that the chiral (Phebim)Ir complexes might also act as effective and stereoselective catalysts for the enantioselective C–H functionalization of indoles with α -aryl- α -diazoacetates. To explore this possibility, we proceeded with the reaction of methyl α -phenyl- α -diazoacetate with *N*-methylindole as the starting point and a model to optimize reaction conditions. The results are shown in Table 1. When the reaction was

Table 1. Enantioselective C–H Insertion of Methyl α -Phenyl- α -diazoacetate with *N*-Methylindole Catalyzed by the (Phebim)Ir Complexes: Optimization of Reaction Conditions^a

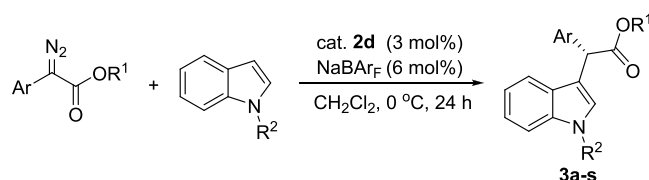


entry	cat. (x mol %)	temp (°C)	solvent	yield (%) ^b	<i>ee</i> (%) ^c
1 ^d	2d (2 mol %)	30	CH ₂ Cl ₂	37	1
2 ^e	2d (2 mol %)	30	CH ₂ Cl ₂	79	31
3 ^e	2d (2 mol %)	20	CH ₂ Cl ₂	79	47
4	2d (2 mol %)	0	CH ₂ Cl ₂	53	84
5 ^f	2d (2 mol %)	0	CH ₂ Cl ₂	54	59
6	2e (2 mol %)	0	CH ₂ Cl ₂	41	22
7	2f (2 mol %)	0	CH ₂ Cl ₂	96	8
8	2g' (2 mol %)	0	CH ₂ Cl ₂	23	23
9	2h (2 mol %)	0	CH ₂ Cl ₂	74	12
10	2d (3 mol %)	0	CH ₂ Cl ₂	86	84
11	2d (3 mol %)	0	DCE	70	81
12	2d (3 mol %)	0	THF	n.d.	

^aReaction conditions: methyl α -phenyl- α -diazoacetate (0.20 mmol), *N*-methylindole (0.24 mmol), cat. **2** (x mol %), NaBARF (2x mol %), solvent (2 mL), Ar, 24 h. ^bIsolated yield. n.d.: not detected. ^cDetermined by chiral HPLC analysis. ^dWithout NaBARF. ^eReaction time was 6 h. ^f100 mg of 4 Å molecular sieves was added.

carried out with 2 mol % of Ir complex **2d** as the catalyst in CH₂Cl₂ at 30 °C for 24 h, one nearly completely racemic product of **3a** was obtained in a 37% yield (entry 1). Importantly, both the yield and enantioselectivity of **3a** were found to increase significantly in the presence of 4 mol % of NaBARF with a reaction time of only 6 h (79% yield with 31% *ee*, entry 2). Under the circumstance of lowering the reaction temperature to 20 °C, a higher enantioselectivity was provided without any loss of activity (79% yield with 47% *ee*, entry 3). When the temperature was further lowered to 0 °C, a high enantioselectivity of 84% *ee* was achieved. However, the activity apparently decreased, and the yield was only 53% after 24 h (entry 4). The addition of 4 Å molecular sieves did not afford any appreciable improvement in yield and instead resulted in a marked drop in enantioselectivity (entry 5). Subsequently, the catalytic potential of (Phebim)Ir complexes **2e–h** was examined. All four complexes gave rather low enantioselectivities (8–23% *ee*), although the yield reached as high as 96% with complex **2f** as the catalyst (entries 6–9 vs entry 4). Upon increasing the amount of complex **2d** and NaBARF to 3 and 6 mol %, respectively, the yield was markedly improved to 86%, whereas the enantioselectivity remained at the highest level of 84% *ee* (entry 10 vs entry 4). Both

Table 2. Enantioselective C–H Insertion of α -Aryl- α -diazoacetates with *N*-Protected Indoles Catalyzed by the (Phebm)Ir Complex **2d^a**



entry	Ar	R ¹	R ²	product	yield (%) ^b	ee (%) ^{c,d}
1	C ₆ H ₅	Me	Me	3a	86	84
2	C ₆ H ₅	Me	Bn	3b	67	74
3	C ₆ H ₅	Me	TBDMS ^e	3c	31	66
4	C ₆ H ₅	Et	Me	3d	47	70
5	C ₆ H ₅	<i>i</i> -Pr	Me	3e	25	71
6	C ₆ H ₅	<i>i</i> -pentyl	Me	3f	42	77
7	C ₆ H ₅	Bn	Me	3g	98	68
8	4-FC ₆ H ₄	Me	Me	3h	87	79
9	4-ClC ₆ H ₄	Me	Me	3i	82	52
10	4-BrC ₆ H ₄	Me	Me	3j	87	46
11	4-MeC ₆ H ₄	Me	Me	3k	66	84
12	4-MeOC ₆ H ₄	Me	Me	3l	41	86
13	3-ClC ₆ H ₄	Me	Me	3m	86	48
14	3-CF ₃ C ₆ H ₄	Me	Me	3n	98	58
15	3-MeOC ₆ H ₄	Me	Me	3o	35	46
16	3,4-Cl ₂ C ₆ H ₃	Me	Me	3p	>99	37
17	3,4-(MeO) ₂ C ₆ H ₃	Me	Me	3q	21	65
18	2-ClC ₆ H ₄	Me	Me	3r	trace	
19	3-thienyl	Me	Me	3s	70	47

^aReaction conditions: α -aryl- α -diazoacetate (0.20 mmol), *N*-protected indole (0.24 mmol), cat. **2d** (3 mol %), NaBAR_F (6 mol %), CH₂Cl₂ (2 mL), 0 °C, 24 h, Ar. ^bIsolated yield. ^cDetermined by chiral HPLC analysis. ^dAbsolute configuration of **3c** was assigned to be *S* by a comparison of its optical rotation with that for the same compound in ref **15a**. The absolute configurations of other products were assigned by analogy. ^eTBDMS, *tert*-butyldimethylsilyl.

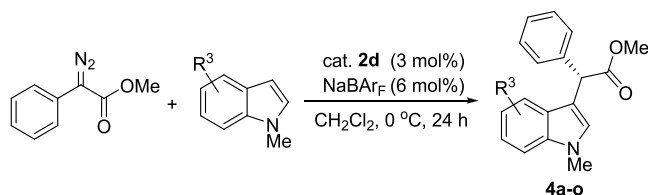
ClCH₂CH₂Cl (DCE) and THF were found to be not ideal solvents for the reaction because the yield and *ee* value decreased when DCE was used, and the reaction did not occur in THF (entries 11 and 12). Thus on the basis of the above data, the optimized conditions for the model reaction include using 3 mol % of complex **2d** as the catalyst in the presence of 6 mol % of NaBAR_F and CH₂Cl₂ as the solvent at a temperature of 0 °C for 24 h.

Under the optimized conditions, the effects of the *N*-protection group (R²) of the indole and ester (alkyl) group (R¹) in α -phenyl- α -diazoacetate on the reactions were investigated (Table 2). In comparison with *N*-methylindole, the *N*-benzyl and *N*-(*tert*-butyldimethylsilyl) indole gave the corresponding products **3b** and **3c** in obviously decreased yields and with decreased enantioselectivities, although the enantioselectivities were still good (entries 1–3). Similar trends were observed when the ester group in α -phenyl- α -diazoacetate was changed from methyl to ethyl, *i*-propyl, and *i*-pentyl (entries 4–6). In the case of benzyl α -phenyl- α -diazoacetate, the enantioselectivity also decreased. However, a very high yield of 98% was obtained (entry 7). The above results indicate that methyl is an appropriate *N*-protection group for indole and also an ideal ester group for α -diazoacetate in the reaction. On the basis of these findings, methyl α -phenyl- α -diazoacetate was extended to methyl α -aryl- α -diazoacetates and then used to react with *N*-methylindole. Overall, substituents with varied electronic properties at the 3-, 4-, and 3,4-positions of the aryl ring were all found to be tolerated, delivering the desired chiral products **3h–q** in good

yields with moderate to good enantioselectivities (37–86% *ee*, entries 8–17). The substituents included both electron-withdrawing groups (F, Cl, Br, and CF₃) and electron-donating groups (Me and OMe). It was found that methyl α -aryl- α -diazoacetates with electron-withdrawing groups generally exhibited higher reactivity than those with electron-donating groups. However, the enantioselectivities were higher with electron-donating groups than with electron-withdrawing groups. Compared with 3-, 4-, and 3,4-substituted methyl α -aryl- α -diazoacetates, the 2-Cl-substituted diazo substrate reacted poorly with *N*-methylindole and afforded only a trace amount of the product (entry 18). Finally, the reaction of the diazo substrate bearing a heteroaryl (thiophen-3-yl) proceeded smoothly to give the product **3s** in 70% yield, albeit with a moderate *ee* value of 47% (entry 19).

To explore further the potential of (Phebm)Ir complex **2d** in the enantioselective C–H functionalization of indoles with α -aryl- α -diazoacetates, reactions of various substituted *N*-methylindoles with methyl α -phenyl- α -diazoacetate were carried out (Table 3). The substituent is located at the C4-, C5-, C6-, or C7-position of the indole ring and can be either an electron-donating group such as Me and OMe or an electron-withdrawing group such as F, Cl, Br, or CO₂Me (entries 1–14). A high *ee* value of 84% accompanied by an excellent yield was achieved only in the case of 6-Me *N*-methylindole (entry 10). For the 4-F, 5-MeO, 5-CO₂Me, and 7-MeO indoles, low enantioselectivities were obtained (6–37% *ee*, entries 2, 8, 9 and 14). For all other reactions, moderate enantioselectivities were observed (43–62% *ee*). Roughly, 4-substituted *N*-

Table 3. Enantioselective C–H Insertion of Methyl α -Phenyl- α -diazoacetate with Substituted *N*-Methylindoles Catalyzed by the (Phebim)Ir Complex 2d^a



entry	R ³	product	yield (%) ^b	ee (%) ^{c,d}
1	4-Me	4a	49	62
2	4-F	4b	47	20
3	4-Cl	4c	44	57
4	5-Me	4d	90	58
5	5-F	4e	73	55
6	5-Cl	4f	36	49
7	5-Br	4g	40	43
8	5-MeO	4h	80	37
9	5-CO ₂ Me	4i	63	35
10	6-Me	4j	96	84
11	6-Cl	4k	32	55
12	6-Br	4l	30	52
13	7-Me	4m	89	54
14	7-MeO	4n	59	6
15 ^e	2-Me	4o	trace	

^aReaction conditions: methyl α -phenyl- α -diazoacetate (0.20 mmol), substituted *N*-methylindole (0.24 mmol), cat. **2d** (3 mol %), NaBARF (6 mol %), CH₂Cl₂ (2 mL), 0 °C, 24 h, Ar. ^bIsolated yield. ^cDetermined by chiral HPLC analysis. ^dAbsolute configurations of the products were assigned by analogy. ^eReaction was carried out at 40 °C.

methylindoles exhibited lower reactivity, possibly due to the steric hindrance at the C4-position. In addition, the *N*-methylindoles with electron-donating groups were generally much more reactive than those with electron-withdrawing groups, which is in direct contrast with the substituent effect in methyl α -aryl- α -diazoacetates. Unfortunately, the reaction of a 2-substituted *N*-methylindole such as 1,2-dimethylindole with methyl α -phenyl- α -diazoacetate at room temperature (~20 °C) failed to afford the desired product (data not shown), and the reaction was very sluggish, even at a temperature of 40 °C (entry 15).

In comparison with the reported Fe, Rh, Pd, and Cu catalytic systems,¹⁵ the current Ir system exhibited generally inferior stereocontrol in the reactions. Nonetheless, in the cases of some specific substrates such as methyl α -aryl- α -diazoacetates bearing a 4-Me or 4-MeO group on the aryl ring, the Ir catalyst could afford comparable^{15b} or better enantioselectivity.^{15a} In addition, the sterically hindered substrates including the diazo compounds with an ortho substituent on the aryl ring (Table 2, entry 18) and 2-substituted *N*-protected indoles (Table 3, entry 15) were almost unreactive under the Ir-catalyzed reaction conditions. For Fe,^{15a} Rh,^{15b} and Cu^{15d} catalysts, the reactions were also sensitive to the steric hindrance of the diazo substrates. However, the desired products could still be obtained in moderate to high yields and with moderate to high enantioselectivities. Interestingly, it was found that in the Pd- and Cu-catalyzed reactions, the presence of a substituent at the indole C2 position was crucial for achieving high levels of enantioselectivity.^{15c,d} The use of 2-unsubstituted indoles such

as *N*-benzyl or *N*-(*tert*-butyldimethylsilyl) indole as the reactants led to significantly decreased enantioselectivity (12–64% ee).

CONCLUSIONS

In summary, we have synthesized a series of new chiral NCN pincer (Phebim)Ir complexes via C–H activation. X-ray single-crystal diffraction analysis reveals that one of the complexes is a coordinatively unsaturated complex that is stabilized by the weak Ir–H agostic interactions. With the assistance of NaBARF, the Ir complex showed good activity and stereocontrol in the asymmetric C–H insertion reaction of α -aryl- α -diazoacetates with *N*-protected indoles, delivering various chiral 3-substituted indoles in good yields with moderate to good enantioselectivities. The (Phebim)Ir complexes are subjects of the ongoing research in our laboratory to explore further their catalytic potentials in asymmetric carbene insertion reactions.

EXPERIMENTAL SECTION

General Procedures. Solvents were dried with standard methods and freshly distilled prior to use if needed. Chiral amino alcohols,¹⁷ α -aryl- α -diazoacetates,¹⁸ *N*-methylindoles, *N*-benzylindole, and *N*-TBDMS indole¹⁹ were prepared according to the literature methods. All other chemicals were used as purchased. ¹H, ¹³C{¹H}, and ¹⁹F NMR spectra were recorded on a Bruker DPX-400 spectrometer with CDCl₃ as the solvent and TMS as an internal standard. Chemical shift multiplicities are represented as follows: s = singlet, d = doublet, t = triplet, q = quartet, hept = heptet, m = multiplet, dd = doublet of doublets, dt = doublet of triplets, app = apparent, br = broad. HRMS was tested on a Waters Q-ToF Micro MS/MS System ESI spectrometer. The enantiomeric excesses of (*R*)- and (*S*)-enantiomers were determined by HPLC analysis over a chiral column with a UV detector. Melting points were measured with a WC-1 instrument and uncorrected. Optical rotations were recorded on a PerkinElmer 341 polarimeter.

Synthesis of Phebim-H Ligands 1a–h. The ligands **1a–h** were synthesized starting from isophthaloyl chloride or 5-(*tert*-butyl)-isophthalic acid according to the procedure we previously reported.⁸ The characterization data of the new ligands **1f–h** are given as follows.

5-*tert*-Butyl-1,3-bis(*S*)-4-isopropyl-1-*p*-tolyl-4,5-dihydro-1H-imidazol-2-yl)benzene (1f). Pale-yellow solid (812.5 mg, 1.52 mmol, 76% based on the 5-(*tert*-butyl)isophthalic acid). Mp 84–86 °C. [α]_D²⁰ = –1.0 (c 0.374, CH₂Cl₂). ¹H NMR (400 MHz, CDCl₃): δ 7.76 (t, *J* = 1.4 Hz, 1H, ArH), 7.28 (d, *J* = 1.3 Hz, 2H, ArH), 6.94 (d, *J* = 8.2 Hz, 4H, NArH), 6.65 (d, *J* = 8.3 Hz, 4H, NArH), 4.14 (app t, *J* = 9.8 Hz, 2H, NCH₂), 4.08–4.02 (m, 2H, NCH), 3.55 (dd, *J* = 7.4, 8.6 Hz, 2H, NCH₂), 2.23 (s, 6H, CH₃), 1.97–1.89 (m, 2H, CH(CH₃)₂), 1.01 (d, *J* = 6.8 Hz, 6H, CH(CH₃)₂), 0.93 (s, 9H, C(CH₃)₃), 0.92 (d, *J* = 5.8 Hz, 6H, CH(CH₃)₂). ¹³C{¹H} NMR (100 MHz, CDCl₃): δ 161.6, 150.2, 140.1, 133.6, 130.1, 129.2, 127.9, 127.0, 123.4, 69.5, 56.2, 34.4, 32.9, 30.6, 20.7, 18.8, 17.7. HRMS (positive ESI): [M + H]⁺ calcd for C₃₆H₄₇N₄: 535.3801. Found: 535.3796.

5-*tert*-Butyl-1,3-bis(*S*)-4-*tert*-butyl-1-*p*-tolyl-4,5-dihydro-1H-imidazol-2-yl)benzene (1g). Pale-yellow solid (733.2 mg, 1.30 mmol, 65% based on the 5-(*tert*-butyl)isophthalic acid). Mp 99–101 °C. [α]_D²⁰ = +30.2 (c 0.860, CH₂Cl₂). ¹H NMR (400 MHz, CDCl₃): δ 7.76 (s, 1H, ArH), 7.32 (d, *J* = 1.5 Hz, 2H, ArH), 6.96 (d, *J* = 8.1 Hz, 4H, NArH), 6.68 (d, *J* = 8.3 Hz, 4H, NArH), 4.20 (app t, *J* = 10.4 Hz, 2H, NCH₂), 3.98 (dd, *J* = 7.1, 11.0 Hz, 2H, NCH), 3.58 (dd, *J* = 7.2, 9.6 Hz, 2H, NCH₂), 2.23 (s, 6H, CH₃), 0.96 (s, 18H, C(CH₃)₃), 0.93 (s, 9H, C(CH₃)₃). ¹³C{¹H} NMR (100 MHz, CDCl₃): δ 161.8, 150.3, 140.0, 134.1, 129.3, 128.2, 127.4, 123.8, 72.6, 55.3, 34.4, 34.3, 30.6, 25.7, 20.8. HRMS (positive ESI): [M + H]⁺ calcd for C₃₈H₅₁N₄: 563.4114, found: 563.4116.

5-*tert*-Butyl-1,3-bis(*S*)-4-benzyl-1-*p*-tolyl-4,5-dihydro-1H-imidazol-2-yl)benzene (1h). Pale-yellow solid (377.8 mg, 0.60 mmol, 30%

based on the 5-(*tert*-butyl)isophthalic acid). Mp 80–82 °C. $[\alpha]_{\text{D}}^{20} = +44.1$ (c 0.400, CH₂Cl₂). ¹H NMR (400 MHz, CDCl₃): δ 7.75 (t, *J* = 1.4 Hz, 1H, ArH), 7.31–7.17 (m, 12H, ArH and PhH), 6.89 (d, *J* = 8.2 Hz, 4H, NArH), 6.49 (d, *J* = 8.3 Hz, 4H, NArH), 4.56–4.48 (m, 2H, NCH), 4.03 (app t, *J* = 9.8 Hz, 2H, NCH₂), 3.62 (dd, *J* = 6.9, 9.5 Hz, 2H, NCH₂), 3.21 (dd, *J* = 4.5, 13.6 Hz, 2H, CH₂Ph), 2.82 (dd, *J* = 8.6, 13.6 Hz, 2H, CH₂Ph), 2.22 (s, 6H, CH₃), 0.94 (s, 9H, C(CH₃)₃). ¹³C{¹H} NMR (100 MHz, CDCl₃): δ 162.0, 150.3, 139.9, 138.2, 133.6, 130.4, 129.5, 129.2, 128.4, 127.9, 126.7, 126.3, 123.2, 64.8, 58.1, 42.2, 34.4, 30.6, 20.7. HRMS (positive ESI): 0.5[M + 2H]²⁺ calcd for C₂₂H₂₄N₂: 316.1939, found: 316.1938.

Synthesis of the NCN Pincer Iridium(III) Complexes 2a–h. Under an argon atmosphere, IrCl₃·3H₂O (77.6 mg, 0.22 mmol), NaHCO₃ (18.5 mg, 0.22 mmol), and the ligand (0.20 mmol) were first dissolved in 6.6 mL of anhydrous alcohol in a dry Schlenk tube. Then, the tube was fitted with a reflux condenser, and the resulting mixture was refluxed for 12 h. The reaction mixture was allowed to cool to room temperature and concentrated *in vacuo*. The residue was purified by chromatography on silica gel plates (for 2a–c and 2g') and further purified by column chromatography on silica gel (for 2d–f and 2h) to give the corresponding bis(imidazoline) NCN pincer iridium(III) complex.

Bis(imidazoline) NCN Pincer Iridium(III) Complex (2a). With CH₂Cl₂/*n*-hexane (5/1) as the eluent; red solid (24.3 mg, 16%). Mp 189–200 °C. $[\alpha]_{\text{D}}^{20} = +215.9$ (c 0.368, CH₂Cl₂). ¹H NMR (400 MHz, CDCl₃): δ 7.21 (d, *J* = 8.3 Hz, 4H, NArH), 7.16 (d, *J* = 8.4 Hz, 4H, NArH), 6.53–6.46 (m, 3H, ArH), 4.39–4.28 (m, 4H, ImH), 3.99 (dd, *J* = 5.3, 8.6 Hz, 2H, ImH), 2.99 (br s, 2H, OH₂), 2.54–2.48 (m, 2H, CH(CH₃)₂), 2.40 (s, 6H, CH₃), 1.00 (d, *J* = 6.7 Hz, 6H, CH(CH₃)₂), 0.97 (d, *J* = 7.0 Hz, 6H, CH(CH₃)₂). ¹³C{¹H} NMR (100 MHz, CDCl₃): δ 170.4, 138.7, 137.0, 133.0, 130.0, 127.4, 126.0, 119.6, 67.7, 55.1, 29.5, 21.1, 19.3, 15.3. Anal. Calcd for C₃₂H₃₉Cl₂IrN₄O: C, 50.65; H, 5.18; N, 7.38. Found: C, 50.49; H, 5.32; N, 7.19.

Bis(imidazoline) NCN Pincer Iridium(III) Complex (2b'). With CH₂Cl₂/*n*-hexane (5/1) as the eluent; red solid (23.1 mg, 15%). Mp > 250 °C. $[\alpha]_{\text{D}}^{20} = +311.0$ (c 0.280, CH₂Cl₂). ¹H NMR (400 MHz, CDCl₃): δ 7.23 (d, *J* = 8.4 Hz, 4H, NArH), 7.20 (d, *J* = 8.5 Hz, 4H, NArH), 6.45–6.37 (m, 3H, ArH), 4.42 (dd, *J* = 9.4, 10.6 Hz, 2H, ImH), 4.19 (app t, *J* = 11.0 Hz, 2H, ImH), 4.03 (dd, *J* = 9.4, 11.0 Hz, 2H, ImH), 2.41 (s, 6H, CH₃), 1.28 (s, 18H, C(CH₃)₃). ¹³C{¹H} NMR (100 MHz, CDCl₃): δ 170.3, 138.7, 137.6, 133.5, 130.2, 127.6, 126.3, 120.0, 72.5, 57.2, 34.1, 27.0, 21.2. Anal. Calcd for C₃₄H₄₁Cl₂IrN₄: C, 53.11; H, 5.38; N, 7.29. Found: C, 53.23; H, 5.65; N, 6.77.

Bis(imidazoline) NCN Pincer Iridium(III) Complex (2c). With CH₂Cl₂/*n*-hexane (5/1) as the eluent; red solid (25.5 mg, 13%). Mp > 250 °C. $[\alpha]_{\text{D}}^{20} = +302.8$ (c 0.385, CH₂Cl₂). ¹H NMR (400 MHz, CDCl₃): δ 7.43–7.42 (m, 4H, PhH), 7.41–7.26 (m, 18H, NArH and PhH), 7.10 (br s, 5H, PhH), 6.82 (br s, 1H, PhH), 6.54–6.45 (m, 3H, ArH), 5.11 (d, *J* = 11.7 Hz, 2H, ImH), 4.88 (d, *J* = 11.7 Hz, 2H, ImH), 2.33 (s, 6H, CH₃), 1.87 (s, 2H, OH₂). ¹³C{¹H} NMR (100 MHz, CDCl₃): δ 179.0, 175.7, 139.3, 139.0, 138.9, 137.9, 133.6, 129.9, 128.74, 128.69, 128.56, 128.48, 128.42, 128.2, 128.1, 119.2, 81.0, 77.2, 21.1. Anal. Calcd for C₅₀H₄₃Cl₂IrN₄O: C, 61.34; H, 4.43; N, 5.72. Found: C, 61.23; H, 4.63; N, 5.28.

Bis(imidazoline) NCN Pincer Iridium(III) Complex (2d). First with CH₂Cl₂/*n*-hexane (3/1), then with CH₂Cl₂/petroleum ether (1/1 to 3/1) as the eluent; red solid (95.2 mg, 46%). Mp > 250 °C. $[\alpha]_{\text{D}}^{20} = +277.3$ (c 0.375, CH₂Cl₂). ¹H NMR (400 MHz, CDCl₃): δ 7.45 (d, *J* = 6.6 Hz, 4H, PhH), 7.39–7.36 (m, 4H, PhH), 7.32–7.24 (m, 13H, NArH and PhH), 7.11 (br s, 5H, PhH), 6.87 (br s, 2H, PhH), 6.41 (s, 2H, ArH), 5.19 (d, *J* = 10.5 Hz, 2H, ImH), 4.97 (d, *J* = 10.5 Hz, 2H, ImH), 2.31 (s, 6H, CH₃), 2.22 (br s, 2H, OH₂), 0.80 (s, 9H, C(CH₃)₃). ¹³C{¹H} NMR (100 MHz, CDCl₃): δ 173.5, 142.2, 139.9, 139.6, 138.1, 132.6, 129.9, 128.8, 128.6, 128.5, 128.4, 128.1, 125.8, 80.3, 76.6, 34.2, 31.1, 21.1. Anal. Calcd for C₅₄H₅₁Cl₂IrN₄O·0.25CH₂Cl₂: C, 61.68; H, 4.91; N, 5.30. Found: C, 61.60; H, 5.13; N, 4.99.

Bis(imidazoline) NCN Pincer Iridium(III) Complex (2e). First with CH₂Cl₂, then with CH₂Cl₂/petroleum ether (1/1) to CH₂Cl₂ as the eluent; red solid (77.7 mg, 44%). Mp 230–232 °C. $[\alpha]_{\text{D}}^{20} = +339.7$ (c 0.475, CH₂Cl₂). ¹H NMR (400 MHz, CDCl₃): δ 7.61 (d, *J* = 7.0 Hz, 4H, PhH), 7.36 (t, *J* = 7.2 Hz, 4H, PhH), 7.31–7.24 (m, 10H, NArH and PhH), 6.58 (s, 2H, ArH), 5.33–5.26 (m, 2H, ImH), 4.63 (app t, *J* = 10.1 Hz, 2H, ImH), 4.04 (dd, *J* = 9.6, 12.1 Hz, 2H, ImH), 2.40 (s, 6H, CH₃), 2.25 (br s, 2H, OH₂), 0.84 (s, 9H, C(CH₃)₃). ¹³C{¹H} NMR (100 MHz, CDCl₃): δ 173.1, 161.3, 141.9, 140.4, 138.4, 137.6, 132.4, 129.9, 128.8, 128.6, 128.2, 126.7, 125.9, 67.1, 63.7, 34.3, 31.2, 21.1. Anal. Calcd for C₄₂H₄₃Cl₂IrN₄O·0.25CH₂Cl₂: C, 56.12; H, 4.85; N, 6.20. Found: C, 55.75; H, 4.90; N, 5.90.

Bis(imidazoline) NCN Pincer Iridium(III) Complex (2f). First with CH₂Cl₂/ethyl acetate (20/1), then with CH₂Cl₂/ethyl acetate (100/1 to 80/1) as the eluent; red solid (73.2 mg, 45%). Mp 183–187 °C. $[\alpha]_{\text{D}}^{20} = +163.0$ (c 0.216, CH₂Cl₂). ¹H NMR (400 MHz, CDCl₃): δ 7.22 (d, *J* = 8.4 Hz, 4H, NArH), 7.18 (d, *J* = 8.3 Hz, 4H, NArH), 6.49 (s, 2H, ArH), 4.38–4.28 (m, 4H, ImH), 4.03 (dd, *J* = 4.5, 7.9 Hz, 2H, ImH), 3.11 (br s, 2H, OH₂), 2.55–2.52 (m, 2H, CH(CH₃)₂), 2.39 (s, 6H, CH₃), 1.01 (d, *J* = 6.6 Hz, 6H, CH(CH₃)₂), 0.97 (d, *J* = 7.0 Hz, 6H, CH(CH₃)₂), 0.81 (s, 9H, C(CH₃)₃). ¹³C{¹H} NMR (100 MHz, CDCl₃): δ 170.6, 142.2, 138.6, 137.1, 132.2, 129.8, 126.4, 125.2, 67.8, 54.8, 34.2, 31.1, 29.6, 21.1, 19.3, 15.3. Anal. Calcd for C₃₆H₄₇Cl₂IrN₄O·C₃H₆O: C, 53.66; H, 6.12; N, 6.42. Found: C, 53.90; H, 6.12; N, 6.42.

Bis(imidazoline) NCN Pincer Iridium(III) Complex (2g'). With CH₂Cl₂ as the eluent; red solid (76.9 mg, 47%). Mp > 250 °C. $[\alpha]_{\text{D}}^{20} = +214.5$ (c 0.552, CH₂Cl₂). ¹H NMR (400 MHz, CDCl₃): δ 7.26–7.21 (m, 8H, NArH), 6.37 (s, 2H, ArH), 4.39 (dd, *J* = 9.2, 10.5 Hz, 2H, ImH), 4.23 (app t, *J* = 11.1 Hz, 2H, ImH), 4.07 (dd, *J* = 9.1, 11.6 Hz, 2H, ImH), 2.40 (s, 6H, CH₃), 1.29 (s, 18H, C(CH₃)₃), 0.78 (s, 9H, C(CH₃)₃). ¹³C{¹H} NMR (100 MHz, CDCl₃): δ 170.3, 143.7, 143.0, 138.5, 137.7, 132.6, 130.0, 126.6, 125.4, 72.6, 56.8, 34.1, 34.0, 31.1, 27.0, 21.1. Anal. Calcd for C₃₈H₄₉Cl₂IrN₄O·0.5CH₂Cl₂: C, 53.31; H, 5.81; N, 6.46. Found: C, 52.81; H, 5.97; N, 6.32.

Bis(imidazoline) NCN Pincer Iridium(III) Complex (2h). First with CH₂Cl₂/ethyl acetate (20/1), then with CH₂Cl₂/ethyl acetate (100/1 to 80/1) as the eluent; red solid (61.5 mg, 34%). Mp 223–225 °C. $[\alpha]_{\text{D}}^{20} = +154.0$ (c 0.150, CH₂Cl₂). ¹H NMR (400 MHz, CDCl₃): δ 7.34–7.11 (m, 18H, PhH and NArH), 6.51 (s, 2H, ArH), 4.67 (br s, 2H, ImH), 4.19 (app t, *J* = 9.8 Hz, 2H, ImH), 3.96–3.91 (m, 2H, ImH), 3.74–3.71 (m, 2H, CH₂Ph), 3.01–2.95 (m, 2H, CH₂Ph), 2.81 (br s, 2H, OH₂), 2.38 (s, 6H, CH₃), 0.82 (s, 9H, C(CH₃)₃). ¹³C{¹H} NMR (100 MHz, CDCl₃): δ 171.3, 142.3, 138.3, 138.2, 137.3, 132.4, 129.7, 129.5, 128.5, 126.5, 126.3, 125.4, 64.1, 59.5, 40.8, 34.2, 31.1, 21.0. Anal. Calcd for C₄₄H₄₇Cl₂IrN₄O: C, 58.01; H, 5.20; N, 6.15. Found: C, 57.76; H, 5.48; N, 6.91.

Typical Procedure for C–H Insertion Reactions of α -Aryl- α -diazoacetates with *N*-Protected Indoles Using the Pincer Ir–Phebin Complex 2d as the Catalyst. Under an argon atmosphere, the pincer Ir–Phebin complex 2d (6.2 mg, 3 mol %) and NaBAR_F (sodium tetrakis[3,5-bis(trifluoromethyl)phenyl]borate), 10.6 mg, 6 mol %) were dissolved in 1.0 mL of CH₂Cl₂ in a dry Schlenk tube, and the mixture was stirred at 30 °C for 2 h. Then, the substrate of *N*-protected indole (0.24 mmol) diluted by CH₂Cl₂ (0.5 mL) was added at room temperature, and the tube was placed at 0 °C. After stirring for a few minutes, α -aryl- α -diazoacetate (0.20 mmol) diluted by CH₂Cl₂ (0.5 mL) was added, and the resulting mixture was stirred at 0 °C for another 24 h. The solvent was evaporated under vacuum, and the residue was purified by chromatography on silica gel plates with petroleum ether/ethyl acetate 20/1 or 5/1 (for 4i) as the eluent to afford products 3 and 4. The enantiomeric excesses were determined by HPLC analysis.

(*S*)-Methyl 2-(1-Methyl-1H-indol-3-yl)-2-phenylacetate (3a).^{15b,18,20} Colorless oil (48.1 mg, 86%). The enantiomeric excess was determined on a Daicel Chiralcel OD-H column with *n*-hexane/2-propanol (90/10) and a flow rate of 1.0 mL/min and detected at a UV wavelength of 254 nm. Retention times: 9.6 min (minor), 12.8 min (major), 84% ee. $[\alpha]_{\text{D}}^{20} = +17.5$ (c 0.690, CH₂Cl₂). ¹H NMR

(400 MHz, CDCl₃): δ 7.45–7.40 (m, 3H), 7.33–7.19 (m, 5H), 7.08–7.04 (m, 2H), 5.26 (s, 1H), 3.75 (s, 3H), 3.74 (s, 3H).

(*S*)-Methyl 2-(1-Benzyl-1*H*-indol-3-yl)-2-phenylacetate (**3b**).^{15b,18} Colorless oil (47.7 mg, 67%). The enantiomeric excess was determined on a Daicel Chiralcel OD-H column with *n*-hexane/2-propanol (90/10) and a flow rate of 1.0 mL/min and detected at a UV wavelength of 254 nm. Retention times: 12.4 min (minor), 21.5 min (major), 74% ee. $[\alpha]_{\text{D}}^{20} = +24.6$ (c 0.886, CH₂Cl₂). ¹H NMR (400 MHz, CDCl₃): δ 7.45–7.41 (m, 3H), 7.33–7.22 (m, 7H), 7.18 (s, 1H), 7.16–7.09 (m, 3H), 7.07–7.03 (m, 1H), 5.30 (s, 2H), 5.28 (s, 1H), 3.74 (s, 3H).

(*S*)-Methyl 2-(1-(*tert*-Butyldimethylsilyl)-1*H*-indol-3-yl)-2-phenylacetate (**3c**).^{15a} Colorless oil (23.4 mg, 31%). The enantiomeric excess was determined on a Daicel Chiralpak AD-H column with *n*-hexane/2-propanol (96/1.2) and a flow rate of 0.8 mL/min and detected at a UV wavelength of 254 nm. Retention times: 6.2 min (minor), 6.9 min (major), 66% ee. $[\alpha]_{\text{D}}^{20} = +36.0$ (c 0.358, CH₂Cl₂). ¹H NMR (400 MHz, CDCl₃): δ 7.48 (d, *J* = 8.3 Hz, 1H), 7.41–7.38 (m, 3H), 7.32–7.28 (m, 2H), 7.24–7.21 (m, 2H), 7.15–7.11 (m, 1H), 7.06–7.02 (m, 1H), 5.25 (s, 1H), 3.74 (s, 3H), 0.92 (s, 9H), 0.592 (s, 3H), 0.586 (s, 3H).

(*S*)-Ethyl 2-(1-Methyl-1*H*-indol-3-yl)-2-phenylacetate (**3d**).^{15b} Colorless oil (27.3 mg, 47%). The enantiomeric excess was determined on a Daicel Chiralcel OD-H column with *n*-hexane/2-propanol (90/10) and a flow rate of 1.0 mL/min and detected at a UV wavelength of 254 nm. Retention times: 9.3 min (minor), 11.0 min (major), 70% ee. $[\alpha]_{\text{D}}^{20} = +17.6$ (c 0.516, CH₂Cl₂). ¹H NMR (400 MHz, CDCl₃): δ 7.46–7.42 (m, 3H), 7.32–7.18 (m, 5H), 7.07–7.04 (m, 2H), 5.23 (s, 1H), 4.26–4.14 (m, 2H), 3.73 (s, 3H), 1.25 (t, *J* = 7.1 Hz, 3H).

(*S*)-Isopropyl 2-(1-Methyl-1*H*-indol-3-yl)-2-phenylacetate (**3e**). Colorless oil (15.3 mg, 25%). The enantiomeric excess was determined on a Daicel Chiralpak AS-H column with *n*-hexane/2-propanol (90/10) and a flow rate of 1.0 mL/min and detected at a UV wavelength of 254 nm. Retention times: 5.9 min (minor), 6.8 min (major), 71% ee. $[\alpha]_{\text{D}}^{20} = +13.0$ (c 0.282, CH₂Cl₂). ¹H NMR (400 MHz, CDCl₃): δ 7.46–7.41 (m, 3H), 7.32–7.18 (m, 5H), 7.07–7.03 (m, 2H), 5.20 (s, 1H), 5.07 (hept, *J* = 6.3 Hz, 1H), 3.73 (s, 3H), 1.24 (d, *J* = 6.3 Hz, 3H), 1.20 (d, *J* = 6.3 Hz, 3H). ¹³C{¹H} NMR (100 MHz, CDCl₃): δ 172.6, 139.0, 137.0, 128.5, 128.4, 127.9, 127.14, 127.09, 121.8, 119.2, 119.1, 112.3, 109.3, 68.5, 49.1, 32.8, 21.8, 21.7. HRMS (positive ESI): [M + H]⁺ calcd for C₂₀H₂₂NO₂: 308.1651, found: 308.1652.

(*S*)-Isopentyl 2-(1-Methyl-1*H*-indol-3-yl)-2-phenylacetate (**3f**). Colorless oil (28.1 mg, 42%). The enantiomeric excess was determined on a Daicel Chiralpak AS-H column with *n*-hexane/2-propanol (90/10) and a flow rate of 1.0 mL/min and detected at a UV wavelength of 254 nm. Retention times: 5.8 min (minor), 6.5 min (major), 77% ee. $[\alpha]_{\text{D}}^{20} = +15.9$ (c 0.520, CH₂Cl₂). ¹H NMR (400 MHz, CDCl₃): δ 7.45–7.41 (m, 3H), 7.32–7.18 (m, 5H), 7.08–7.03 (m, 2H), 5.23 (s, 1H), 4.22–4.12 (m, 2H), 3.74 (s, 3H), 1.66–1.56 (m, 1H), 1.54–1.48 (m, 2H), 0.87 (d, *J* = 6.5 Hz, 3H), 0.86 (d, *J* = 6.6 Hz, 3H). ¹³C{¹H} NMR (100 MHz, CDCl₃): δ 173.2, 138.9, 137.0, 128.5, 128.4, 127.9, 127.2, 127.1, 121.8, 119.2, 119.1, 112.2, 109.3, 63.8, 49.0, 37.3, 32.8, 25.0, 22.4. HRMS (positive ESI): [M + H]⁺ calcd for C₂₂H₂₆NO₂: 336.1964, found: 336.1963.

(*S*)-Benzyl 2-(1-Methyl-1*H*-indol-3-yl)-2-phenylacetate (**3g**).^{15b} Colorless oil (69.9 mg, 98%). The enantiomeric excess was determined on a Daicel Chiralcel OD-H column with *n*-hexane/2-propanol (95/5) and a flow rate of 1.0 mL/min and detected at a UV wavelength of 254 nm. Retention times: 19.4 min (minor), 21.2 min (major), 68% ee. $[\alpha]_{\text{D}}^{20} = +16.6$ (c 1.302, CH₂Cl₂). ¹H NMR (400 MHz, CDCl₃): δ 7.42–7.39 (m, 3H), 7.33–7.18 (m, 10H), 7.05–7.00 (m, 2H), 5.30 (s, 1H), 5.21 (d, *J* = 12.4 Hz, 1H), 5.16 (d, *J* = 12.4 Hz, 1H), 3.73 (s, 3H).

(*S*)-Methyl 2-(4-Fluorophenyl)-2-(1-methyl-1*H*-indol-3-yl)acetate (**3h**). Colorless oil (51.9 mg, 87%). The enantiomeric excess was determined on a Daicel Chiralcel OD-H column with *n*-hexane/2-propanol (90/10) and a flow rate of 1.0 mL/min and detected at a UV wavelength of 254 nm. Retention times: 10.4 min (minor), 15.0

min (major), 79% ee. $[\alpha]_{\text{D}}^{20} = +33.9$ (c 0.620, CH₂Cl₂). ¹H NMR (400 MHz, CDCl₃): δ 7.41–7.36 (m, 3H), 7.30 (d, *J* = 8.2 Hz, 1H), 7.24–7.20 (m, 1H), 7.08–7.05 (m, 2H), 7.02–6.96 (m, 2H), 5.23 (s, 1H), 3.77 (s, 3H), 3.75 (s, 3H). ¹³C{¹H} NMR (100 MHz, CDCl₃): δ 173.4, 162.1 (d, ¹*J*_{C-F} = 244.1 Hz), 137.1, 134.5 (d, ⁴*J*_{C-F} = 3.1 Hz), 130.0 (d, ³*J*_{C-F} = 8.0 Hz), 127.8, 126.9, 122.0, 119.4, 119.0, 115.4 (d, ²*J*_{C-F} = 21.4 Hz), 111.9, 109.5, 52.4, 48.0, 32.8. ¹⁹F NMR (376 MHz, CDCl₃): δ -115.6. HRMS (positive ESI): [M + H]⁺ calcd for C₁₈H₁₇FNO₂: 298.1243, found: 298.1244.

(*S*)-Methyl 2-(4-Chlorophenyl)-2-(1-methyl-1*H*-indol-3-yl)acetate (**3i**).^{15b} Colorless oil (51.3 mg, 82%). The enantiomeric excess was determined on a Daicel Chiralcel OD-H column with *n*-hexane/2-propanol (90/10) and a flow rate of 1.0 mL/min and detected at a UV wavelength of 254 nm. Retention times: 10.8 min (minor), 16.5 min (major), 52% ee. $[\alpha]_{\text{D}}^{20} = +10.8$ (c 1.016, CH₂Cl₂). ¹H NMR (400 MHz, CDCl₃): δ 7.40 (d, *J* = 8.0 Hz, 1H), 7.36–7.34 (m, 2H), 7.31–7.25 (m, 3H), 7.23–7.20 (m, 1H), 7.08–7.04 (m, 2H), 5.22 (m, 1H), 3.76 (s, 3H), 3.75 (s, 3H).

(*S*)-Methyl 2-(4-Bromophenyl)-2-(1-methyl-1*H*-indol-3-yl)acetate (**3j**).^{15b} Colorless oil (62.5 mg, 87%). The enantiomeric excess was determined on a Daicel Chiralcel OD-H column with *n*-hexane/2-propanol (90/10) and a flow rate of 1.0 mL/min and detected at a UV wavelength of 254 nm. Retention times: 12.2 min (minor), 17.8 min (major), 46% ee. $[\alpha]_{\text{D}}^{20} = +5.7$ (c 1.290, CH₂Cl₂). ¹H NMR (400 MHz, CDCl₃): δ 7.44–7.38 (m, 3H), 7.31–7.28 (m, 3H), 7.24–7.20 (m, 1H), 7.08–7.04 (m, 2H), 5.21 (s, 1H), 3.76 (s, 3H), 3.75 (s, 3H).

(*S*)-Methyl 2-(1-Methyl-1*H*-indol-3-yl)-2-(*p*-tolyl)acetate (**3k**).^{15b} Colorless oil (38.9 mg, 66%). The enantiomeric excess was determined on a Daicel Chiralcel OD-H column with *n*-hexane/2-propanol (90/10) and a flow rate of 1.0 mL/min and detected at a UV wavelength of 254 nm. Retention times: 9.1 min (minor), 13.9 min (major), 84% ee. $[\alpha]_{\text{D}}^{20} = +8.5$ (c 0.758, CH₂Cl₂). ¹H NMR (400 MHz, CDCl₃): δ 7.44 (d, *J* = 7.9 Hz, 1H), 7.31–7.27 (m, 3H), 7.22–7.18 (m, 1H), 7.12 (d, *J* = 7.9 Hz, 2H), 7.08–7.03 (m, 2H), 5.22 (s, 1H), 3.75 (s, 3H), 3.73 (s, 3H), 2.32 (s, 3H).

(*S*)-Methyl 2-(4-Methoxyphenyl)-2-(1-methyl-1*H*-indol-3-yl)acetate (**3l**).^{15b} Colorless oil (25.2 mg, 41%). The enantiomeric excess was determined on a Daicel Chiralcel OD-H column with *n*-hexane/2-propanol (90/10) and a flow rate of 1.0 mL/min and detected at a UV wavelength of 254 nm. Retention times: 16.5 min (minor), 24.7 min (major), 86% ee. $[\alpha]_{\text{D}}^{20} = +10.3$ (c 0.532, CH₂Cl₂). ¹H NMR (400 MHz, CDCl₃): δ 7.43 (d, *J* = 8.0 Hz, 1H), 7.35–7.32 (m, 2H), 7.29 (d, *J* = 8.2 Hz, 1H), 7.23–7.18 (m, 1H), 7.08–7.03 (m, 2H), 6.86–6.83 (m, 2H), 5.20 (s, 1H), 3.78 (s, 3H), 3.75 (s, 3H), 3.74 (s, 3H).

(*S*)-Methyl 2-(3-Chlorophenyl)-2-(1-methyl-1*H*-indol-3-yl)acetate (**3m**).^{15b} Colorless oil (54.1 mg, 86%). The enantiomeric excess was determined on a Daicel Chiralcel OD-H column with *n*-hexane/2-propanol (90/10) and a flow rate of 1.0 mL/min and detected at a UV wavelength of 254 nm. Retention times: 11.1 min (minor), 19.1 min (major), 48% ee. $[\alpha]_{\text{D}}^{20} = +17.7$ (c 0.928, CH₂Cl₂). ¹H NMR (400 MHz, CDCl₃): δ 7.42 (d, *J* = 7.9 Hz, 2H), 7.31–7.29 (m, 2H), 7.24–7.20 (m, 3H), 7.09–7.06 (m, 2H), 5.23 (s, 1H), 3.78 (s, 3H), 3.75 (s, 3H).

(*S*)-Methyl 2-(1-Methyl-1*H*-indol-3-yl)-2-(3-(trifluoromethyl)phenyl)acetate (**3n**). Colorless oil (68.1 mg, 98%). The enantiomeric excess was determined on a Daicel Chiralcel OD-H column with *n*-hexane/2-propanol (90/10) and a flow rate of 1.0 mL/min and detected at a UV wavelength of 254 nm. Retention times: 9.7 min (minor), 20.7 min (major), 58% ee. $[\alpha]_{\text{D}}^{20} = +27.0$ (c 1.234, CH₂Cl₂). ¹H NMR (400 MHz, CDCl₃): δ 7.70 (s, 1H), 7.61 (d, *J* = 7.8 Hz, 1H), 7.52 (d, *J* = 7.8 Hz, 1H), 7.44–7.41 (m, 2H), 7.31 (d, *J* = 8.2 Hz, 1H), 7.25–7.21 (m, 1H), 7.10–7.06 (m, 2H), 5.31 (s, 1H), 3.78 (s, 3H), 3.76 (s, 3H). ¹³C{¹H} NMR (100 MHz, CDCl₃): δ 173.0, 139.8, 137.1, 131.9, 130.8 (q, ²*J*_{C-F} = 31.9 Hz), 129.0, 127.9, 126.8, 125.3 (q, ³*J*_{C-F} = 3.7 Hz), 124.23 (q, ³*J*_{C-F} = 3.8 Hz), 124.15 (q, ¹*J*_{C-F} = 270.7 Hz), 122.1, 119.5, 118.8, 111.2, 109.5, 52.5, 48.6, 32.9. ¹⁹F NMR (376 MHz, CDCl₃): δ -62.4. HRMS (positive ESI): [M + H]⁺ calcd for C₁₉H₁₇F₃NO₂: 348.1211, found: 348.1212.

(*S*)-Methyl 2-(3-Methoxyphenyl)-2-(1-methyl-1*H*-indol-3-yl)-acetate (**3o**).^{15b} Colorless oil (21.5 mg, 35%). The enantiomeric excess was determined on a Daicel Chiralcel OD-H column with *n*-hexane/2-propanol (90/10) and a flow rate of 1.0 mL/min and detected at a UV wavelength of 254 nm. Retention times: 13.6 min (minor), 19.4 min (major), 46% ee. $[\alpha]_D^{20} = +4.9$ (c 0.428, CH₂Cl₂). ¹H NMR (400 MHz, CDCl₃): δ 7.46 (d, *J* = 8.0 Hz, 1H), 7.28 (d, *J* = 8.2 Hz, 1H), 7.23–7.19 (m, 2H), 7.08–7.05 (m, 2H), 7.01 (d, *J* = 7.8 Hz, 1H), 6.99–6.98 (m, 1H), 6.81–6.78 (m, 1H), 5.23 (s, 1H), 3.77 (s, 3H), 3.75 (s, 3H), 3.74 (s, 3H).

(*S*)-Methyl 2-(3,4-Dichlorophenyl)-2-(1-methyl-1*H*-indol-3-yl)-acetate (**3p**). Colorless oil (69.3 mg, >99%). The enantiomeric excess was determined on a Daicel Chiralcel OD-H column with *n*-hexane/2-propanol (90/10) and a flow rate of 1.0 mL/min and detected at a UV wavelength of 254 nm. Retention times: 12.1 min (minor), 22.2 min (major), 37% ee. $[\alpha]_D^{20} = +12.1$ (c 1.342, CH₂Cl₂). ¹H NMR (400 MHz, CDCl₃): δ 7.50 (d, *J* = 2.1 Hz, 1H), 7.40–7.36 (m, 2H), 7.31 (d, *J* = 8.2 Hz, 1H), 7.25–7.21 (m, 2H), 7.10–7.06 (m, 2H), 5.20 (s, 1H), 3.78 (s, 3H), 3.76 (s, 3H). ¹³C{¹H} NMR (100 MHz, CDCl₃): δ 172.7, 139.1, 137.1, 132.6, 131.4, 130.4, 127.9, 127.8, 126.7, 122.2, 119.6, 118.8, 110.8, 109.5, 52.6, 47.9, 32.9. HRMS (positive ESI): [M + H]⁺ calcd for C₁₈H₁₆Cl₂NO₂: 348.0558, found: 348.0556.

(*S*)-Methyl 2-(3,4-Dimethoxyphenyl)-2-(1-methyl-1*H*-indol-3-yl)-acetate (**3q**). Colorless oil (14.3 mg, 21%). The enantiomeric excess was determined on a Daicel Chiralcel OD-H column with *n*-hexane/2-propanol (90/10) and a flow rate of 1.0 mL/min and detected at a UV wavelength of 254 nm. Retention times: 17.5 min (minor), 25.6 min (major), 65% ee. $[\alpha]_D^{20} = +3.0$ (c 0.258, CH₂Cl₂). ¹H NMR (400 MHz, CDCl₃): δ 7.45 (d, *J* = 8.0 Hz, 1H), 7.29 (d, *J* = 8.2 Hz, 1H), 7.23–7.19 (m, 1H), 7.09–7.05 (m, 1H), 7.00 (s, 1H), 6.98–6.95 (m, 2H), 6.81 (d, *J* = 8.0 Hz, 1H), 5.19 (s, 1H), 3.86 (s, 3H), 3.83 (s, 3H), 3.76 (s, 3H), 3.75 (s, 3H). ¹³C{¹H} NMR (100 MHz, CDCl₃): δ 173.7, 148.9, 148.2, 137.1, 131.1, 127.8, 127.0, 121.9, 120.6, 119.3, 119.0, 112.4, 111.6, 111.0, 109.4, 55.91, 55.89, 52.3, 48.4, 32.8. HRMS (positive ESI): [M + Na]⁺ calcd for C₂₀H₂₁NNaO₄: 362.1368, found: 362.1367.

(*R*)-Methyl 2-(1-Methyl-1*H*-indol-3-yl)-2-(thiophen-3-yl)acetate (**3s**). Colorless oil (39.7 mg, 70%). The enantiomeric excess was determined on a Daicel Chiralcel OD-H column with *n*-hexane/2-propanol (90/10) and a flow rate of 1.0 mL/min and detected at a UV wavelength of 254 nm. Retention times: 11.8 min (minor), 16.0 min (major), 47% ee. $[\alpha]_D^{20} = +4.0$ (c 0.728, CH₂Cl₂). ¹H NMR (400 MHz, CDCl₃): δ 7.53 (d, *J* = 8.0 Hz, 1H), 7.30–7.20 (m, 4H), 7.12 (dd, *J* = 1.2, 4.9 Hz, 1H), 7.09–7.07 (m, 1H), 6.99 (s, 1H), 5.33 (s, 1H), 3.75 (s, 3H), 3.74 (s, 3H). ¹³C{¹H} NMR (100 MHz, CDCl₃): δ 173.2, 139.0, 137.1, 128.0, 127.8, 126.9, 125.6, 122.5, 121.9, 119.4, 119.2, 112.0, 109.4, 52.4, 44.3, 32.8. HRMS (positive ESI): [M + H]⁺ calcd for C₁₆H₁₆NO₂S: 286.0902, found: 286.0901.

(*S*)-Methyl 2-(1,4-Dimethyl-1*H*-indol-3-yl)-2-phenylacetate (**4a**). Colorless oil (28.9 mg, 49%). The enantiomeric excess was determined on a Daicel Chiralcel OD-H column with *n*-hexane/2-propanol (90/10) and a flow rate of 1.0 mL/min and detected at a UV wavelength of 254 nm. Retention times: 10.0 min (minor), 12.0 min (major), 62% ee. $[\alpha]_D^{20} = +22.0$ (c 0.592, CH₂Cl₂). ¹H NMR (400 MHz, CDCl₃): δ 7.35–7.22 (m, 5H), 7.13–7.06 (m, 2H), 6.97 (s, 1H), 6.79 (d, *J* = 6.8 Hz, 1H), 5.61 (s, 1H), 3.74 (s, 3H), 3.70 (s, 3H), 2.54 (s, 3H). ¹³C{¹H} NMR (100 MHz, CDCl₃): δ 174.1, 139.6, 137.5, 130.5, 128.6, 128.5, 127.2, 125.8, 121.9, 121.2, 112.4, 107.4, 52.4, 49.7, 33.0, 20.4. HRMS (positive ESI): [M + H]⁺ calcd for C₁₉H₂₀NO₂: 294.1494, found: 294.1496.

(*S*)-Methyl 2-(4-Fluoro-1-methyl-1*H*-indol-3-yl)-2-phenylacetate (**4b**). Colorless oil (28.1 mg, 47%). The enantiomeric excess was determined on a Daicel Chiralcel OD-H column with *n*-hexane/2-propanol (90/10) and a flow rate of 1.0 mL/min and detected at a UV wavelength of 254 nm. Retention times: 7.9 min (minor), 9.4 min (major), 20% ee. $[\alpha]_D^{20} = -8.4$ (c 0.570, CH₂Cl₂). ¹H NMR (400 MHz, CDCl₃): δ 7.42 (d, *J* = 7.4 Hz, 2H), 7.35–7.31 (m, 2H), 7.28–7.23 (m, 1H), 7.11–7.06 (m, 1H), 7.02 (d, *J* = 8.2 Hz, 1H), 6.86 (s, 1H), 6.74–6.69 (m, 1H), 5.45 (s, 1H), 3.73 (s, 3H), 3.68 (s, 3H).

¹³C{¹H} NMR (100 MHz, CDCl₃): δ 173.7, 157.0 (d, ¹J_{C-F} = 244.5 Hz), 139.7 (d, ³J_{C-F} = 11.7 Hz), 138.8, 128.7, 128.4, 128.1, 127.3, 122.3 (d, ³J_{C-F} = 7.8 Hz), 115.8 (d, ²J_{C-F} = 19.6 Hz), 111.5 (d, ³J_{C-F} = 3.4 Hz), 105.6 (d, ⁴J_{C-F} = 3.5 Hz), 104.5 (d, ²J_{C-F} = 19.6 Hz), 52.4, 49.3 (d, *J*_{C-F} = 2.0 Hz), 33.2. ¹⁹F NMR (376 MHz, CDCl₃): δ -123.5. HRMS (positive ESI): [M + H]⁺ calcd for C₁₈H₁₇FNO₂: 298.1243, found: 298.1245.

(*S*)-Methyl 2-(4-Chloro-1-methyl-1*H*-indol-3-yl)-2-phenylacetate (**4c**). Colorless oil (27.3 mg, 44%). The enantiomeric excess was determined on a Daicel Chiralcel OD-H column with *n*-hexane/2-propanol (90/10) and a flow rate of 1.0 mL/min and detected at a UV wavelength of 254 nm. Retention times: 9.3 min (minor), 10.9 min (major), 57% ee. $[\alpha]_D^{20} = +34.1$ (c 0.522, CH₂Cl₂). ¹H NMR (400 MHz, CDCl₃): δ 7.39–7.23 (m, 5H), 7.16–7.03 (m, 3H), 6.79 (s, 1H), 5.85 (s, 1H), 3.74 (s, 3H), 3.67 (s, 3H). ¹³C{¹H} NMR (100 MHz, CDCl₃): δ 174.1, 139.0, 138.5, 129.9, 128.7, 128.6, 127.2, 126.0, 123.9, 122.3, 120.4, 113.0, 108.3, 52.4, 48.9, 33.1. HRMS (positive ESI): [M + H]⁺ calcd for C₁₈H₁₇ClNO₂: 314.0948, found: 314.0949.

(*S*)-Methyl 2-(1,5-Dimethyl-1*H*-indol-3-yl)-2-phenylacetate (**4d**).²⁰ Colorless oil (53.0 mg, 90%). The enantiomeric excess was determined on a Daicel Chiralcel OD-H column with *n*-hexane/2-propanol (98/2) and a flow rate of 0.8 mL/min and detected at a UV wavelength of 254 nm. Retention times: 19.1 min (minor), 21.1 min (major), 58% ee. $[\alpha]_D^{20} = +4.2$ (c 1.002, CH₂Cl₂). ¹H NMR (400 MHz, CDCl₃): δ 7.43–7.40 (m, 2H), 7.33–7.29 (m, 2H), 7.27–7.22 (m, 2H), 7.17 (d, *J* = 8.4 Hz, 1H), 7.03 (dd, *J* = 1.4, 8.3 Hz, 1H), 6.99 (s, 1H), 5.23 (s, 1H), 3.74 (s, 3H), 3.72 (s, 3H), 2.40 (s, 3H).

(*S*)-Methyl 2-(5-Fluoro-1-methyl-1*H*-indol-3-yl)-2-phenylacetate (**4e**). Colorless oil (43.6 mg, 73%). The enantiomeric excess was determined on a Daicel Chiralcel OD-H column with *n*-hexane/2-propanol (98/1.4) and a flow rate of 1.0 mL/min and detected at a UV wavelength of 254 nm. Retention times: 20.5 min (minor), 22.3 min (major), 55% ee. $[\alpha]_D^{20} = +6.6$ (c 0.790, CH₂Cl₂). ¹H NMR (400 MHz, CDCl₃): δ 7.41–7.39 (m, 2H), 7.33–7.23 (m, 3H), 7.17 (dd, *J* = 4.3, 8.9 Hz, 1H), 7.08–7.05 (m, 2H), 6.94 (dt, *J* = 2.4, 9.1 Hz, 1H), 5.16 (s, 1H), 3.74 (s, 3H), 3.72 (s, 3H). ¹³C{¹H} NMR (100 MHz, CDCl₃): δ 173.3, 157.8 (d, ¹J_{C-F} = 233.2 Hz), 138.4, 133.7, 129.5, 128.7, 128.3, 127.4, 127.2 (d, ³J_{C-F} = 9.6 Hz), 112.0 (d, ⁴J_{C-F} = 4.6 Hz), 110.3 (d, ²J_{C-F} = 26.4 Hz), 110.1 (d, ³J_{C-F} = 10.2 Hz), 104.1 (d, ²J_{C-F} = 23.7 Hz), 52.4, 48.8, 33.1. ¹⁹F NMR (376 MHz, CDCl₃): δ -124.8. HRMS (positive ESI): [M + H]⁺ calcd for C₁₈H₁₇FNO₂: 298.1243, found: 298.1244.

(*S*)-Methyl 2-(5-Chloro-1-methyl-1*H*-indol-3-yl)-2-phenylacetate (**4f**).²⁰ Colorless oil (22.6 mg, 36%). The enantiomeric excess was determined on a Daicel Chiralpak AD-H column with *n*-hexane/2-propanol (98/2) and a flow rate of 1.0 mL/min and detected at a UV wavelength of 254 nm. Retention times: 15.9 min (major), 18.1 min (minor), 49% ee. $[\alpha]_D^{20} = -9.5$ (c 0.442, CH₂Cl₂). ¹H NMR (400 MHz, CDCl₃): δ 7.40–7.38 (m, 3H), 7.34–7.24 (m, 3H), 7.20–7.13 (m, 2H), 7.07 (s, 1H), 5.18 (s, 1H), 3.75 (s, 3H), 3.73 (s, 3H).

(*S*)-Methyl 2-(5-Bromo-1-methyl-1*H*-indol-3-yl)-2-phenylacetate (**4g**).¹⁸ Colorless oil (28.4 mg, 40%). The enantiomeric excess was determined on a Daicel Chiralpak AD-H column with *n*-hexane/2-propanol (90/10) and a flow rate of 1.0 mL/min and detected at a UV wavelength of 254 nm. Retention times: 8.4 min (major), 9.5 min (minor), 43% ee. $[\alpha]_D^{20} = -13.2$ (c 0.522, CH₂Cl₂). ¹H NMR (400 MHz, CDCl₃): δ 7.56 (d, *J* = 1.8 Hz, 1H), 7.41–7.38 (m, 2H), 7.34–7.25 (m, 4H), 7.14 (d, *J* = 8.7 Hz, 1H), 7.06 (s, 1H), 5.18 (s, 1H), 3.75 (s, 3H), 3.73 (s, 3H).

(*S*)-Methyl 2-(5-Methoxy-1-methyl-1*H*-indol-3-yl)-2-phenylacetate (**4h**).^{15b,20} Colorless oil (49.3 mg, 80%). The enantiomeric excess was determined on a Daicel Chiralpak AD-H column with *n*-hexane/2-propanol (90/10) and a flow rate of 1.0 mL/min and detected at a UV wavelength of 254 nm. Retention times: 12.5 min (minor), 15.7 min (major), 37% ee. $[\alpha]_D^{20} = -1.4$ (c 0.962, CH₂Cl₂). ¹H NMR (400 MHz, CDCl₃): δ 7.43–7.41 (m, 2H), 7.33–7.23 (m, 3H), 7.18–7.15 (m, 1H), 7.00 (s, 1H), 6.88–6.85 (m, 2H), 5.20 (s, 1H), 3.78 (s, 3H), 3.74 (s, 3H), 3.72 (s, 3H).

(*S*)-Methyl 3-(2-Methoxy-2-oxo-1-phenylethyl)-1-methyl-1*H*-indole-5-carboxylate (**4i**). Colorless oil (42.3 mg, 63%). The enantiomeric excess was determined on a Daicel Chiralpak AD-H column with *n*-hexane/2-propanol (90/10) and a flow rate of 1.0 mL/min and detected at a UV wavelength of 254 nm. Retention times: 15.7 min (major), 19.8 min (minor), 35% ee. $[\alpha]_{\text{D}}^{20} = -17.7$ (c 0.582, CH₂Cl₂). ¹H NMR (400 MHz, CDCl₃): δ 8.24 (d, *J* = 1.1 Hz, 1H), 7.91 (dd, *J* = 1.6, 8.7 Hz, 1H), 7.44–7.41 (m, 2H), 7.34–7.24 (m, 4H), 7.12 (s, 1H), 5.30 (s, 1H), 3.90 (s, 3H), 3.75 (s, 6H). ¹³C{¹H} NMR (100 MHz, CDCl₃): δ 173.3, 168.1, 139.4, 138.4, 129.4, 128.7, 128.3, 127.4, 126.7, 123.3, 121.9, 121.4, 113.9, 109.1, 52.4, 51.9, 48.4, 33.0. HRMS (positive ESI): [M + H]⁺ calcd for C₂₀H₂₀NO₄: 338.1392, found: 338.1391.

(*S*)-Methyl 2-(1,6-Dimethyl-1*H*-indol-3-yl)-2-phenylacetate (**4j**).^{15b} Colorless oil (56.6 mg, 96%). The enantiomeric excess was determined on a Daicel Chiralcel OD-H column with *n*-hexane/2-propanol (90/10) and a flow rate of 1.0 mL/min and detected at a UV wavelength of 254 nm. Retention times: 8.2 min (major), 9.7 min (minor), 84% ee. $[\alpha]_{\text{D}}^{20} = +19.6$ (c 1.098, CH₂Cl₂). ¹H NMR (400 MHz, CDCl₃): δ 7.42–7.39 (m, 2H), 7.32–7.22 (m, 4H), 7.08 (s, 1H), 6.96 (s, 1H), 6.89 (dd, *J* = 0.9, 8.1 Hz, 1H), 5.23 (s, 1H), 3.74 (s, 3H), 3.71 (s, 3H), 2.46 (s, 3H).

(*S*)-Methyl 2-(6-Chloro-1-methyl-1*H*-indol-3-yl)-2-phenylacetate (**4k**).^{15b} Colorless oil (19.9 mg, 32%). The enantiomeric excess was determined on a Daicel Chiralpak IC column with *n*-hexane/2-propanol (90/10) and a flow rate of 1.0 mL/min and detected at a UV wavelength of 254 nm. Retention times: 6.6 min (major), 7.2 min (minor), 55% ee. $[\alpha]_{\text{D}}^{20} = +8.4$ (c 0.350, CH₂Cl₂). ¹H NMR (400 MHz, CDCl₃): δ 7.40–7.37 (m, 2H), 7.33–7.23 (m, 5H), 7.03–6.99 (m, 2H), 5.20 (s, 1H), 3.74 (s, 3H), 3.69 (s, 3H).

(*S*)-Methyl 2-(6-Bromo-1-methyl-1*H*-indol-3-yl)-2-phenylacetate (**4l**). Colorless oil (21.3 mg, 30%). The enantiomeric excess was determined on a Daicel Chiralcel OD-H column with *n*-hexane/2-propanol (98/1.4) and a flow rate of 1.0 mL/min and detected at a UV wavelength of 254 nm. Retention times: 18.0 min (major), 19.7 min (minor), 52% ee. $[\alpha]_{\text{D}}^{20} = +5.8$ (c 0.384, CH₂Cl₂). ¹H NMR (400 MHz, CDCl₃): δ 7.43 (d, *J* = 1.6 Hz, 1H), 7.39–7.37 (m, 2H), 7.33–7.23 (m, 4H), 7.14 (dd, *J* = 1.6, 8.5 Hz, 1H), 7.02 (d, *J* = 0.4 Hz, 1H), 5.20 (s, 1H), 3.74 (s, 3H), 3.70 (s, 3H). ¹³C{¹H} NMR (100 MHz, CDCl₃): δ 173.3, 138.4, 137.9, 128.6, 128.5, 128.3, 127.4, 125.9, 122.5, 120.4, 115.6, 112.45, 112.42, 52.4, 48.7, 32.9. HRMS (positive ESI): [M + Na]⁺ calcd for C₁₈H₁₆BrNNO₂: 380.0262, found: 380.0261.

(*S*)-Methyl 2-(1,7-Dimethyl-1*H*-indol-3-yl)-2-phenylacetate (**4m**).^{15b} Colorless oil (52.0 mg, 89%). The enantiomeric excess was determined on a Daicel Chiralcel OD-H column with *n*-hexane/2-propanol (90/10) and a flow rate of 1.0 mL/min and detected at a UV wavelength of 254 nm. Retention times: 9.7 min (minor), 18.8 min (major), 54% ee. $[\alpha]_{\text{D}}^{20} = +20.3$ (c 0.908, CH₂Cl₂). ¹H NMR (400 MHz, CDCl₃): δ 7.42–7.39 (m, 2H), 7.33–7.22 (m, 4H), 6.93–6.87 (m, 3H), 5.21 (s, 1H), 4.01 (s, 3H), 3.74 (s, 3H), 2.74 (s, 3H).

(*S*)-Methyl 2-(7-Methoxy-1-methyl-1*H*-indol-3-yl)-2-phenylacetate (**4n**). Colorless oil (36.4 mg, 59%). The enantiomeric excess was determined on a Daicel Chiralpak IC column with *n*-hexane/2-propanol (90/10) and a flow rate of 1.0 mL/min and detected at a UV wavelength of 254 nm. Retention times: 10.9 min (major), 12.9 min (minor), 6% ee. $[\alpha]_{\text{D}}^{20} = +2.1$ (c 0.658, CH₂Cl₂). ¹H NMR (400 MHz, CDCl₃): δ 7.41–7.39 (m, 2H), 7.31–7.27 (m, 2H), 7.25–7.21 (m, 1H), 7.00 (dd, *J* = 0.9, 8.0 Hz, 1H), 6.93–6.90 (m, 2H), 6.57 (d, *J* = 7.6 Hz, 1H), 5.20 (s, 1H), 3.99 (s, 3H), 3.87 (s, 3H), 3.72 (s, 3H). ¹³C{¹H} NMR (100 MHz, CDCl₃): δ 173.6, 147.9, 138.8, 129.3, 128.9, 128.6, 128.4, 127.2, 126.8, 119.8, 112.0, 111.8, 102.7, 55.4, 52.3, 48.8, 36.5. HRMS (positive ESI): [M + Na]⁺ calcd for C₁₉H₁₉NNaO₃: 332.1263, found: 332.1261.

X-ray Diffraction Studies. Crystals of **2c**, **2d**, and **2g'** (CCDCs 1915664, 1905111, and 1953152) suitable for X-ray single-crystal analysis were obtained by recrystallization at ambient temperature from CH₂Cl₂/*n*-hexane, toluene, and CH₂Cl₂/*n*-hexane, respectively. The data were collected on an Oxford diffraction Gemini E

diffractometer with graphite-monochromated Cu K α radiation ($\lambda = 1.54184 \text{ \AA}$) at ambient temperature. The structures were solved by direct methods using the SHELXS-97 program, and all non-hydrogen atoms were refined anisotropically on F^2 by the full-matrix least-squares technique, using the SHELXL-97 crystallographic software package.²¹ The hydrogen atoms were included but not refined. Additional details of X-ray diffraction studies are provided in the Supporting Information.

ASSOCIATED CONTENT

Supporting Information

The Supporting Information is available free of charge at <https://pubs.acs.org/doi/10.1021/acs.organomet.0c00174>.

Crystallographic details of the Ir(III) complexes **2c**, **2d**, and **2g'**. NMR spectra of the new ligands **1f–h**, complexes **2a–h**, and catalysis products **3** and **4** as well as their chiral HPLC spectra (PDF)

Accession Codes

CCDC 1905111, 1915664, and 1953152 contain the supplementary crystallographic data for this paper. These data can be obtained free of charge via www.ccdc.cam.ac.uk/data_request/cif, or by emailing data_request@ccdc.cam.ac.uk, or by contacting The Cambridge Crystallographic Data Centre, 12 Union Road, Cambridge CB2 1EZ, UK; fax: +44 1223 336033.

AUTHOR INFORMATION

Corresponding Authors

Jun-Fang Gong – College of Chemistry, Henan Key Laboratory of Chemical Biology and Organic Chemistry, Green Catalysis Center, Zhengzhou University, Zhengzhou 450001, People's Republic of China; orcid.org/0000-0002-5299-1323; Phone: (+86)-371-6776-3869; Email: gongjf@zzu.edu.cn

Mao-Ping Song – College of Chemistry, Henan Key Laboratory of Chemical Biology and Organic Chemistry, Green Catalysis Center, Zhengzhou University, Zhengzhou 450001, People's Republic of China; orcid.org/0000-0003-3883-2622; Email: mpsong@zzu.edu.cn

Authors

Nan Li – College of Chemistry, Henan Key Laboratory of Chemical Biology and Organic Chemistry, Green Catalysis Center, Zhengzhou University, Zhengzhou 450001, People's Republic of China

Wen-Jing Zhu – College of Chemistry, Henan Key Laboratory of Chemical Biology and Organic Chemistry, Green Catalysis Center, Zhengzhou University, Zhengzhou 450001, People's Republic of China

Juan-Juan Huang – College of Chemistry, Henan Key Laboratory of Chemical Biology and Organic Chemistry, Green Catalysis Center, Zhengzhou University, Zhengzhou 450001, People's Republic of China

Xin-Qi Hao – College of Chemistry, Henan Key Laboratory of Chemical Biology and Organic Chemistry, Green Catalysis Center, Zhengzhou University, Zhengzhou 450001, People's Republic of China; orcid.org/0000-0003-1942-8309

Complete contact information is available at:

<https://pubs.acs.org/doi/10.1021/acs.organomet.0c00174>

Notes

The authors declare no competing financial interest.

ACKNOWLEDGMENTS

This research was supported by a grant from the National Natural Science Foundation of China (21472176).

REFERENCES

- (1) For reviews, see: (a) Choi, J.; MacArthur, A. H. R.; Brookhart, M.; Goldman, A. S. Dehydrogenation and Related Reactions Catalyzed by Iridium Pincer Complexes. *Chem. Rev.* **2011**, *111*, 1761–1779. (b) Haibach, M. C.; Kundu, S.; Brookhart, M.; Goldman, A. S. Alkane Metathesis by Tandem Alkane-Dehydrogenation-Olefin-Metathesis Catalysis and Related Chemistry. *Acc. Chem. Res.* **2012**, *45*, 947–958. (c) Hackenberg, J.; Krogh-Jespersen, K.; Goldman, A. S. Activation of C–O and C–F Bonds by Pincer-iridium Complexes. In *Advances in Organometallic Chemistry and Catalysis: The Silver/Gold Jubilee International Conference on Organometallic Chemistry Celebratory Book*; Pombreiro, A. J. L., Ed.; John Wiley & Sons, Inc.: Hoboken, NJ, 2014; Chapter 4, pp 39–57. (d) Werkmeister, S.; Neumann, J.; Junge, K.; Beller, M. Pincer-Type Complexes for Catalytic (De)Hydrogenation and Transfer (De)Hydrogenation Reactions: Recent Progress. *Chem. - Eur. J.* **2015**, *21*, 12226–12250. (e) Kumar, A.; Goldman, A. S. Recent Advances in Alkane Dehydrogenation Catalyzed by Pincer Complexes. *Top. Organomet. Chem.* **2015**, *54*, 307–334. (f) Bézier, D.; Brookhart, M. Transfer Dehydrogenations of Alkanes and Related Reactions Using Iridium Pincer Complexes. *Top. Organomet. Chem.* **2015**, *56*, 189–207. (g) Kumar, A.; Bhatti, T. M.; Goldman, A. S. Dehydrogenation of Alkanes and Aliphatic Groups by Pincer-Ligated Metal Complexes. *Chem. Rev.* **2017**, *117*, 12357–12384. (h) Goldberg, K. I.; Goldman, A. S. Large-Scale Selective Functionalization of Alkanes. *Acc. Chem. Res.* **2017**, *50*, 620–626. (i) Tang, X.; Jia, X.; Huang, Z. Challenges and opportunities for alkane functionalisation using molecular catalysts. *Chem. Sci.* **2018**, *9*, 288–299. (j) Tang, X.; Huang, Z. Transition-metal complex-catalyzed alkane functionalization (in Chinese). *Kexue Tongbao* **2018**, *63*, 1348–1360. (k) Das, K.; Kumar, A. Alkane dehydrogenation reactions catalyzed by pincer-metal complexes. *Adv. Organomet. Chem.* **2019**, *72*, 1–57.
- (2) For selected examples, see: (a) Ito, J.-i.; Kaneda, T.; Nishiyama, H. Intermolecular C–H Bond Activation of Alkanes and Arenes by NCN Pincer Iridium(III) Acetate Complexes Containing Bis-(oxazolonyl)phenyl Ligands. *Organometallics* **2012**, *31*, 4442–4449. (b) Ahuja, R.; Punji, B.; Findlater, M.; Supplee, C.; Schinski, W.; Brookhart, M.; Goldman, A. S. Catalytic dehydroaromatization of *n*-alkanes by pincer-ligated iridium complexes. *Nat. Chem.* **2011**, *3*, 167–171. (c) Kundu, S.; Choi, J.; Wang, D. Y.; Chohly, Y.; Emge, T. J.; Krogh-Jespersen, K.; Goldman, A. S. Cleavage of Ether, Ester, and Tosylate C(sp³)-O Bonds by an Iridium Complex, Initiated by Oxidative Addition of C–H Bonds. Experimental and Computational Studies. *J. Am. Chem. Soc.* **2013**, *135*, 5127–5143. (d) Haibach, M. C.; Guan, C.; Wang, D. Y.; Li, B.; Lease, N.; Steffens, A. M.; Krogh-Jespersen, K.; Goldman, A. S. Olefin Hydroaryloxylation Catalyzed by Pincer-Iridium Complexes. *J. Am. Chem. Soc.* **2013**, *135*, 15062–15070. (e) Cheng, C.; Kim, B. G.; Guironnet, D.; Brookhart, M.; Guan, C.; Wang, D. Y.; Krogh-Jespersen, K.; Goldman, A. S. Synthesis and Characterization of Carbazolide-Based Iridium PNP Pincer Complexes. Mechanistic and Computational Investigation of Alkene Hydrogenation: Evidence for an Ir(III)/Ir(V)/Ir(III) Catalytic Cycle. *J. Am. Chem. Soc.* **2014**, *136*, 6672–6683. (f) Hackenberg, J. D.; Kundu, S.; Emge, T. J.; Krogh-Jespersen, K.; Goldman, A. S. Acid-Catalyzed Oxidative Addition of a C–H Bond to a Square Planar d⁸ Iridium Complex. *J. Am. Chem. Soc.* **2014**, *136*, 8891–8894. (g) Yao, W.; Zhang, Y.; Jia, X.; Huang, Z. Selective Catalytic Transfer Dehydrogenation of Alkanes and Heterocycles by an Iridium Pincer Complex. *Angew. Chem., Int. Ed.* **2014**, *53*, 1390–1394. (h) Haibach, M. C.; Lease, N.; Goldman, A. S. Catalytic Cleavage of Ether C–O Bonds by Pincer Iridium Complexes. *Angew. Chem., Int. Ed.* **2014**, *53*, 10160–10163. (i) Guo, L.; Ma, X.; Fang, H.; Jia, X.; Huang, Z. A General and Mild Catalytic α -Alkylation of Unactivated Esters Using Alcohols. *Angew. Chem., Int. Ed.* **2015**, *54*, 4023–4027. (j) Kumar, A.; Zhou, T.; Emge, T. J.; Mironov, O.; Saxton, R. J.; Krogh-Jespersen, K.; Goldman, A. S. Dehydrogenation of *n*-Alkanes by Solid-Phase Molecular Pincer-Iridium Catalysts. High Yields of α -Olefin Product. *J. Am. Chem. Soc.* **2015**, *137*, 9894–9911. (k) Labinger, J. A.; Leitch, D. C.; Bercaw, J. E.; Deimund, M. A.; Davis, M. E. Upgrading Light Hydrocarbons: A Tandem Catalytic System for Alkane/Alkene Coupling. *Top. Catal.* **2015**, *58*, 494–501. (l) Jia, X.; Huang, Z. Conversion of alkanes to linear alkylsilanes using an iridium-iron-catalysed tandem dehydrogenation-isomerization-hydrosilylation. *Nat. Chem.* **2016**, *8*, 157–161. (m) Wang, Y.; Qin, C.; Jia, X.; Leng, X.; Huang, Z. An Agostic Iridium Pincer Complex as a Highly Efficient and Selective Catalyst for Monoisomerization of 1-Alkenes to *trans*-2-Alkenes. *Angew. Chem., Int. Ed.* **2017**, *56*, 1614–1618. (n) Tang, X.; Jia, X.; Huang, Z. Thermal, Catalytic Conversion of Alkanes to Linear Aldehydes and Linear Amines. *J. Am. Chem. Soc.* **2018**, *140*, 4157–4163. (o) Wang, Y.; Huang, Z.; Leng, X.; Zhu, H.; Liu, G.; Huang, Z. Transfer Hydrogenation of Alkenes Using Ethanol Catalyzed by a NCP Pincer Iridium Complex: Scope and Mechanism. *J. Am. Chem. Soc.* **2018**, *140*, 4417–4429.
- (3) (a) Allen, K. E.; Heinekey, D. M.; Goldman, A. S.; Goldberg, K. I. Alkane Dehydrogenation by C–H Activation at Iridium(III). *Organometallics* **2013**, *32*, 1579–1582. (b) Allen, K. E.; Heinekey, D. M.; Goldman, A. S.; Goldberg, K. I. Regeneration of an Iridium(III) Complex Active for Alkane Dehydrogenation Using Molecular Oxygen. *Organometallics* **2014**, *33*, 1337–1340. (c) d) Zhou, M.; Johnson, S. I.; Gao, Y.; Emge, T. J.; Nielsen, R. J.; Goddard, W. A., III; Goldman, A. S. Activation and Oxidation of Mesitylene C–H Bonds by (Phebox)Iridium(III) Complexes. *Organometallics* **2015**, *34*, 2879–2888. (d) Gao, Y.; Guan, C.; Zhou, M.; Kumar, A.; Emge, T. J.; Wright, A. M.; Goldberg, K. I.; Krogh-Jespersen, K.; Goldman, A. S. β -Hydride Elimination and C–H Activation by an Iridium Acetate Complex, Catalyzed by Lewis Acids. Alkane Dehydrogenation Cocatalyzed by Lewis Acids and [2,6-Bis(4,4-dimethylloxazolonyl)-3,5-dimethylphenyl]iridium. *J. Am. Chem. Soc.* **2017**, *139*, 6338–6350. (e) Yuan, H.; Brennessel, W. W.; Jones, W. D. Effect of Carboxylate Ligands on Alkane Dehydrogenation with (^{dm}Phebox)Ir Complexes. *ACS Catal.* **2018**, *8*, 2326–2329. (f) Syed, Z. H.; Kaphan, D. M.; Perras, F. A.; Pruski, M.; Ferrandon, M. S.; Wegener, E. C.; Celik, G.; Wen, J.; Liu, C.; Dogan, F.; Goldberg, K. I.; Delferro, M. Electrophilic Organoiridium(III) Pincer Complexes on Sulfated Zirconia for Hydrocarbon Activation and Functionalization. *J. Am. Chem. Soc.* **2019**, *141*, 6325–6337.
- (4) Ito, J.-i.; Shiomi, T.; Nishiyama, H. Efficient Preparation of New Rhodium- and Iridium-[Bis(oxazolonyl)-3,5-dimethylphenyl] Complexes by C–H Bond Activation: Applications in Asymmetric Synthesis. *Adv. Synth. Catal.* **2006**, *348*, 1235–1240.
- (5) For reviews on chiral transition-metal pincer complexes with Phebox ligands, see: (a) Nishiyama, H. Synthesis and use of bisoxazolonyl-phenyl pincers. *Chem. Soc. Rev.* **2007**, *36*, 1133–1141. (b) Nishiyama, H.; Ito, J.-i. Bis(oxazolonyl)phenyl transition-metal complexes: asymmetric catalysis and some reactions of the metals. *Chem. Commun.* **2010**, *46*, 203–212. (c) Ito, J.-i.; Nishiyama, H. Synthetic Utility of Chiral Bis(oxazolonyl)phenyl Transition-Metal Complexes. *Synlett* **2012**, *23*, 509–523. (d) Ito, J.-i.; Nishiyama, H. Optically Active Bis(oxazolonyl)phenyl Metal Complexes as Multipotent Catalysts. *Top. Organomet. Chem.* **2013**, *40*, 243–270. (e) Ito, J.-i.; Nishiyama, H. Asymmetric Catalysis Mediated by Optically Active Bis(oxazolonyl)phenyl Metal Complexes. *Yuki Gosei Kagaku Kyokaiishi* **2013**, *71*, 791–803.
- (6) Owens, C. P.; Varela-Álvarez, A.; Boyarskikh, V.; Musaev, D. G.; Davies, H. M. L.; Blakey, S. B. Iridium(III)-bis(oxazolonyl)phenyl catalysts for enantioselective C–H functionalization. *Chem. Sci.* **2013**, *4*, 2590–2596.
- (7) For reviews, see: (a) Niu, J.-L.; Hao, X.-Q.; Gong, J.-F.; Song, M.-P. Symmetrical and unsymmetrical pincer complexes with group 10 metals: synthesis *via* aryl C–H activation and some catalytic applications. *Dalton Trans.* **2011**, *40*, 5135–5150. (b) Hao, X.-Q.; Niu, J.-L.; Zhao, X.-M.; Gong, J.-F.; Song, M.-P. Development of Pincer Catalysts with Selected Group 8–10 Metals. *Youji Huaxue*

- 2013, 33, 663–674. (c) Gong, J.-F.; Zhu, X.; Song, M.-P. Transition Metal Pincer Complexes with Chiral Imidazoline Donor(s): Synthesis and Asymmetric Catalysis. In *Pincer Compounds: Chemistry and Applications*; Morales-Morales, D., Ed.; Elsevier: Amsterdam, 2018; Chapter 9, pp 191–218. (d) Liu, J.-K.; Gong, J.-F.; Song, M.-P. Chiral palladium pincer complexes for asymmetric catalytic reactions. *Org. Biomol. Chem.* 2019, 17, 6069–6098.
- (8) (a) Hao, X.-Q.; Gong, J.-F.; Du, C.-X.; Wu, L.-Y.; Wu, Y.-J.; Song, M.-P. Synthesis, characterization and photoluminescent properties of platinum complexes with novel bis(imidazoline) pincer ligands. *Tetrahedron Lett.* 2006, 47, 5033–5036. (b) Wu, L.-Y.; Hao, X.-Q.; Xu, Y.-X.; Jia, M.-Q.; Wang, Y.-N.; Gong, J.-F.; Song, M.-P. Chiral NCN Pincer Pt(II) and Pd(II) Complexes with 1,3-Bis(2'-imidazolyl)benzene: Synthesis via Direct Metalation, Characterization, and Catalytic Activity in the Friedel-Crafts Alkylation Reaction. *Organometallics* 2009, 28, 3369–3380. (c) Shao, D.-D.; Niu, J.-L.; Hao, X.-Q.; Gong, J.-F.; Song, M.-P. Neutral and cationic chiral NCN pincer nickel(II) complexes with 1,3-bis(2'-imidazolyl)benzenes: synthesis and characterization. *Dalton Trans.* 2011, 40, 9012–9019. (d) Hao, X.-Q.; Xu, Y.-X.; Yang, M.-J.; Wang, L.; Niu, J.-L.; Gong, J.-F.; Song, M.-P. A Cationic NCN Pincer Platinum(II) Aquo Complex with a Bis(imidazolyl)phenyl Ligand: Studies toward its Synthesis and Asymmetric Friedel-Crafts Alkylation of Indoles with Nitroalkenes. *Organometallics* 2012, 31, 835–846. (e) Wang, T.; Niu, J.-L.; Liu, S.-L.; Huang, J.-J.; Gong, J.-F.; Song, M.-P. Chiral NCN Pincer Rhodium(III) Complexes with Bis(imidazolyl)phenyl Ligands: Synthesis and Enantioselective Catalytic Alkynylation of Trifluoropyruvates with Terminal Alkynes. *Adv. Synth. Catal.* 2013, 355, 927–937. (f) Wang, T.; Hao, X.-Q.; Huang, J.-J.; Niu, J.-L.; Gong, J.-F.; Song, M.-P. Chiral Bis(imidazolyl)phenyl NCN Pincer Rhodium(III) Catalysts for Enantioselective Allylation of Aldehydes and Carbonyl-Ene Reaction of Trifluoropyruvates. *J. Org. Chem.* 2013, 78, 8712–8721. (g) Hao, X.-Q.; Zhao, Y.-W.; Yang, J.-J.; Niu, J.-L.; Gong, J.-F.; Song, M.-P. Enantioselective Hydrophosphination of Enones with Diphenylphosphine Catalyzed by Bis(imidazoline) NCN Pincer Palladium(II) Complexes. *Organometallics* 2014, 33, 1801–1811.
- (9) Li, C.; Bian, Q.-L.; Xu, S.; Duan, W.-L. Palladium-catalyzed 1,4-addition of secondary alkylphenylphosphines to α,β -unsaturated carbonyl compounds for the synthesis of phosphorus- and carbon-stereogenic compounds. *Org. Chem. Front.* 2014, 1, 541–545.
- (10) For reviews, see: (a) Nakamura, S. Enantioselective Reaction Using Palladium Pincer Complexes with C_2 -Symmetric Chiral Bis(imidazoline)s. *Yuki Gosei Kagaku Kyokaiishi* 2015, 73, 1062–1071. (b) Hyodo, K.; Nakamura, S. Chiral NCN Pincer-Type Catalysts Having Bis(imidazoline)s. In *Pincer Compounds: Chemistry and Applications*; Morales-Morales, D., Ed.; Elsevier: Amsterdam, 2018; Chapter 10, pp 219–235. For selected examples, see: (c) Nakamura, S.; Hyodo, K.; Nakamura, M.; Nakane, D.; Masuda, H. Catalytic Enantioselective Allylation of Ketimines by Using Palladium Pincer Complexes with Chiral Bis(imidazoline)s. *Chem. - Eur. J.* 2013, 19, 7304–7309. (d) Hyodo, K.; Nakamura, S.; Shibata, N. Enantioselective Aza-Morita-Baylis-Hillman Reactions of Acrylonitrile Catalyzed by Palladium(II) Pincer Complexes having C_2 -Symmetric Chiral Bis(imidazoline) Ligands. *Angew. Chem., Int. Ed.* 2012, 51, 10337–10341. (e) Kondo, M.; Nishi, T.; Hatanaka, T.; Funahashi, Y.; Nakamura, S. Catalytic Enantioselective Reaction of α -Aminoacetonitriles Using Chiral Bis(imidazoline) Palladium Catalysts. *Angew. Chem., Int. Ed.* 2015, 54, 8198–8202. (f) Kondo, M.; Omori, M.; Hatanaka, T.; Funahashi, Y.; Nakamura, S. Catalytic Enantioselective Reaction of Allenyl nitriles with Imines Using Chiral Bis(imidazoline)s Palladium(II) Pincer Complexes. *Angew. Chem., Int. Ed.* 2017, 56, 8677–8680. (g) Kondo, M.; Saito, H.; Nakamura, S. Direct catalytic enantioselective Mannich-type reaction of α,α -dithioacetonitriles with imines using chiral bis(imidazoline)-Pd complexes. *Chem. Commun.* 2017, 53, 6776–6779. (h) Nakamura, S.; Tokunaga, A.; Saito, H.; Kondo, M. Enantioselective conjugate addition of an α,α -dithioacetonitrile with nitroalkenes using chiral bis(imidazoline)-Pd complexes. *Chem. Commun.* 2019, 55, 5391–5394.
- (11) Weldy, N. M.; Schafer, A. G.; Owens, C. P.; Herting, C. J.; Varela-Alvarez, A.; Chen, S.; Niemeyer, Z.; Musaev, D. G.; Sigman, M. S.; Davies, H. M. L.; Blakey, S. B. Iridium(III)-bis(imidazolyl)phenyl catalysts for enantioselective C-H functionalization with ethyl diazoacetate. *Chem. Sci.* 2016, 7, 3142–3146.
- (12) (a) Schultz, K. M.; Goldberg, K. I.; Gusev, D. G.; Heinekey, D. M. Synthesis, Structure, and Reactivity of Iridium NHC Pincer Complexes. *Organometallics* 2011, 30, 1429–1437. (b) Gyton, M. R.; Leforestier, B.; Chaplin, A. B. Rhodium(III) and Iridium(III) Complexes of a NHC-Based Macrocyclic: Persistent Weak Agostic Interactions and Reactions with Dihydrogen. *Organometallics* 2018, 37, 3963–3971. (c) Hood, T. M.; Leforestier, B.; Gyton, M. R.; Chaplin, A. B. Synthesis and Structural Dynamics of Five-Coordinate Rh(III) and Ir(III) PNP and PONOP Pincer Complexes. *Inorg. Chem.* 2019, 58, 7593–7601.
- (13) (a) Brookhart, M.; Green, M. L. H.; Parkin, G. Agostic interactions in transition metal compounds. *Proc. Natl. Acad. Sci. U. S. A.* 2007, 104, 6908–6914. (b) Lein, M. Characterization of agostic interactions in theory and computation. *Coord. Chem. Rev.* 2009, 253, 625–634.
- (14) For reviews, see: (a) Davies, H. M. L.; Beckwith, R. E. J. Catalytic Enantioselective C-H Activation by Means of Metal-Carbenoid-Induced C-H Insertion. *Chem. Rev.* 2003, 103, 2861–2903. (b) Slattery, C. N.; Ford, A.; Maguire, A. R. Catalytic asymmetric C-H insertion reactions of α -diazo carbonyl compounds. *Tetrahedron* 2010, 66, 6681–6705. (c) Zhu, S.-F.; Zhou, Q.-L. Transition-Metal-Catalyzed Enantioselective Heteroatom-Hydrogen Bond Insertion Reactions. *Acc. Chem. Res.* 2012, 45, 1365–1377. (d) Zheng, C.; You, S.-L. Recent development of direct asymmetric functionalization of inert C-H bonds. *RSC Adv.* 2014, 4, 6173–6214. (e) Ren, Y.-Y.; Zhu, S.-F.; Zhou, Q.-L. Chiral proton-transfer shuttle catalysts for carbene insertion reactions. *Org. Biomol. Chem.* 2018, 16, 3087–3094.
- (15) (a) Cai, Y.; Zhu, S.-F.; Wang, G.-P.; Zhou, Q.-L. Iron-Catalyzed C-H Functionalization of Indoles. *Adv. Synth. Catal.* 2011, 353, 2939–2944. (b) Qiu, H.; Zhang, D.; Liu, S.; Qiu, L.; Zhou, J.; Qian, Y.; Zhai, C.; Hu, W. Asymmetric C-H Functionalization of Indoles via Enantioselective Protonation. *Huaxue Xuebao* 2012, 70, 2484–2488. (c) Gao, X.; Wu, B.; Huang, W.-X.; Chen, M.-W.; Zhou, Y.-G. Enantioselective Palladium-Catalyzed C-H Functionalization of Indoles Using an Axially Chiral 2,2'-Bipyridine Ligand. *Angew. Chem., Int. Ed.* 2015, 54, 11956–11960. (d) Gao, X.; Wu, B.; Yan, Z.; Zhou, Y.-G. Copper-catalyzed enantioselective C-H functionalization of indoles with an axially chiral bipyridine ligand. *Org. Biomol. Chem.* 2016, 14, 8237–8240.
- (16) For Ir-catalyzed asymmetric carbene insertion into C-H and X-H bonds, see: (a) Suematsu, H.; Katsuki, T. Iridium(III) Catalyzed Diastereo- and Enantioselective C-H Bond Functionalization. *J. Am. Chem. Soc.* 2009, 131, 14218–14219. (b) Yasutomi, Y.; Suematsu, H.; Katsuki, T. Iridium(III)-Catalyzed Enantioselective Si-H Bond Insertion and Formation of an Enantioenriched Silicon Center. *J. Am. Chem. Soc.* 2010, 132, 4510–4511. (c) Wang, J.-C.; Xu, Z.-J.; Guo, Z.; Deng, Q.-H.; Zhou, C.-Y.; Wan, X.-L.; Che, C.-M. Highly enantioselective intermolecular carbene insertion to C-H and Si-H bonds catalyzed by a chiral iridium(III) complex of a D_4 -symmetric Halterman porphyrin ligand. *Chem. Commun.* 2012, 48, 4299–4301. (d) Wang, J.-C.; Zhang, Y.; Xu, Z.-J.; Lo, V. K.-Y.; Che, C.-M. Enantioselective Intramolecular Carbene C-H Insertion Catalyzed by a Chiral Iridium(III) Complex of D_4 -Symmetric Porphyrin Ligand. *ACS Catal.* 2013, 3, 1144–1148. (e) Schafer, A. G.; Blakey, S. B. Ir-Catalyzed enantioselective group transfer reactions. *Chem. Soc. Rev.* 2015, 44, 5969–5980.
- (17) McKennon, M. J.; Meyers, A. I.; Drauz, K.; Schwarm, M. A Convenient Reduction of Amino Acids and Their Derivatives. *J. Org. Chem.* 1993, 58, 3568–3571.
- (18) Fraile, J. M.; Le Jeune, K.; Mayoral, J. A.; Ravaio, N.; Zacheria, F. CuO/SiO₂ as a simple, effective and recoverable catalyst

for alkylation of indole derivatives with diazo compounds. *Org. Biomol. Chem.* **2013**, *11*, 4327–4332.

(19) Xu, X.-H.; Liu, G.-K.; Azuma, A.; Tokunaga, E.; Shibata, N. Synthesis of Indole and Biindolyl Triflones: Trifluoromethanesulfonylation of Indoles with TF_2O /TTBP (2,4,6-tri-*tert*-butylpyridine) System. *Org. Lett.* **2011**, *13*, 4854–4857.

(20) Sarkar, M.; Daw, P.; Ghatak, T.; Bera, J. K. Amide-Functionalized Naphthyridines on a $\text{Rh}^{\text{II}}\text{-Rh}^{\text{II}}$ Platform: Effect of Steric Crowding, Hemilability, and Hydrogen-Bonding Interactions on the Structural Diversity and Catalytic Activity of Dirhodium(II) Complexes. *Chem. - Eur. J.* **2014**, *20*, 16537–16549.

(21) (a) Sheldrick, G. M. *SHELXS-97, Program for Crystal Structure Solution*; University of Göttingen: Göttingen, Germany, 1997.

(b) Sheldrick, G. M. *SHELXL-97, Program for Crystal Structure Refinement*; University of Göttingen: Göttingen, Germany, 1997.